https://doi.org/10.1093/plcell/koad281 THE PLANT CELL 2024: 36: 688–708

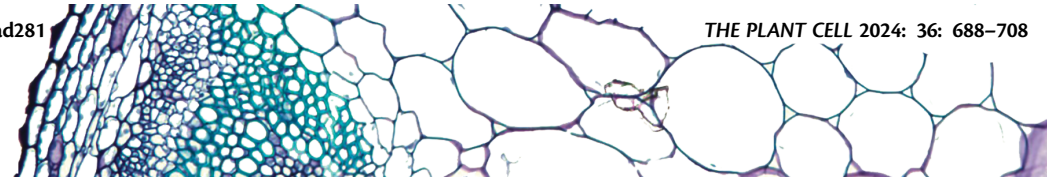

Research Article

H_2O_2 negatively regulates aluminum resistance via oxidation and degradation of the transcription factor STOP1

Xiang Wei [1,2,†] Yifang Zhu [1,†] Wenxiang Xie [1] Weiwei Ren [3] Yang Zhang [1] Hui Zhang [3] Shaojun Dai [3] and Chao-Feng Huang [1,2,*]

1 National Key Laboratory of Plant Molecular Genetics, Key Laboratory of Plant Design, Shanghai Center for Plant Stress Biology, Center for Excellence in Molecular Plant Sciences, Chinese Academy of Sciences, Shanghai 200032, China
2 University of the Chinese Academy of Sciences, Beijing 100049, China
3 Development Center of Plant Germplasm Resources and Shanghai Key Laboratory of Plant Molecular Sciences, College of Life Sciences, Shanghai Normal University, Shanghai 200234, China

*Author for correspondence: huancf@cemps.ac.cn
†These authors contributed equally to this work.
The author responsible for distribution of materials integral to the findings presented in this article in accordance with the policy described in the Instructions for Authors (https://academic.oup.com/plcell/pages/General-Instructions) is: Chao-Feng Huang (huangcf@cemps.ac.cn).

Abstract

Aluminum (Al) stress triggers the accumulation of hydrogen peroxide (H_2O_2) in roots. However, whether H_2O_2 plays a regulatory role in aluminum resistance remains unclear. In this study, we show that H_2O_2 plays a crucial role in regulation of Al resistance, which is modulated by the mitochondrion-localized pentatricopeptide repeat protein REGULATION OF ALMT1 EXPRESSION 6 (RAE6). Mutation in *RAE6* impairs the activity of complex I of the mitochondrial electron transport chain, resulting in the accumulation of H_2O_2 and increased sensitivity to Al. Our results suggest that higher H_2O_2 concentrations promote the oxidation of SENSITIVE TO PROTON RHIZOTOXICITY 1 (STOP1), an essential transcription factor that promotes Al resistance, thereby promoting its degradation by enhancing the interaction between STOP1 and the F-box protein RAE1. Conversely, decreasing H_2O_2 levels or blocking the oxidation of STOP1 leads to greater STOP1 stability and increased Al resistance. Moreover, we show that the thioredoxin TRX1 interacts with STOP1 to catalyze its chemical reduction. Thus, our results highlight the importance of H_2O_2 in Al resistance and regulation of STOP1 stability in Arabidopsis (*Arabidopsis thaliana*).

Introduction

In acids soils, a portion of aluminum (Al) becomes solubilized into trivalent Al (Al^{3+}), which can be toxic to root tip cells, inhibiting root growth and ultimately decreasing plant production. Since acid soils make up over 30% of world's arable land, Al toxicity has been recognized as the second most significant abiotic limitation to crop production, exceeded only by drought stress (von Uexkull and Mutert 1995; Kochian et al. 2015).

The phytotoxic Al^{3+} ion interacts strongly with oxygen donor compounds that contain carboxyl or phosphate groups, allowing it to target various sites in root cells for its toxicity, including the cell wall, plasma membrane, and symplastic components (Kochian 1995; Ma 2007; Poschenrieder et al. 2008). One early symptom and response to Al stress is the accumulation of reactive oxygen species (ROS) such as hydrogen peroxide (H_2O_2) in root tips, which has been observed several plant species, including pea (*Pisum sativum*) (Matsumoto and Motoda 2013), rice (*Oryza sativa*) (Ma et al. 2007), barley (*Hordeum vulgare*) (Tamas et al. 2004), and *Melaleuca* trees (Tahara et al. 2008). In non-photosynthesizing root cells, the mitochondrial electron

Received June 20, 2023. Accepted October 11, 2023. Advance access publication November 4, 2023

IN A NUTSHELL

Background: Aluminum (Al) toxicity limits crop production on acid soils. The exposure of plants to Al stress triggers the accumulation of hydrogen peroxide (H_2O_2) in their roots. To combat Al toxicity, plants use the crucial transcription factor SENSITIVE TO PROTON RHIZOTOXICITY 1 (STOP1), which controls Al resistance. STOP1 undergoes various post-translational modifications, such ubiquitination, SUMOylation, and phosphorylation, to regulate its function.

Question: We wished to understand whether H_2O_2 plays a role in regulating Al signaling and Al resistance by affecting STOP1 through post-translational oxidation.

Findings: We identified the specific protein REGULATION OF ALMT1 EXPRESSION 6 (RAE6), which localizes to mitochondria and contains pentatricopeptide repeats. The mutation of *RAE6* disrupted the activity of complex I in the mitochondrial electron transport chain. This defect led to increased accumulation of H_2O_2 in mitochondria and rendered *rae6* seedlings more sensitive to Al toxicity. We determined that H_2O_2 promotes the oxidation of STOP1 at specific cysteine residues (C8, C27, and C185), which triggers its degradation by enhancing its interaction with the F-box protein RAE1. However, to counteract the negative effects of H_2O_2 on STOP1, another protein, thioredoxin TRX1, can interact with STOP1 and reverse its oxidation.

Next steps: While we learned that H_2O_2 negatively regulates the accumulation of STOP1, it is not the signal that activates another pathway composed of a series of kinases (the MEKK1–MKK1/1–MPK4 cascade), which positively promotes STOP1 accumulation via its phosphorylation. Further research is needed to understand how plants sense Al stress and transmit the signal to the MEKK1–MKK1/1–MPK4 cascade, ultimately leading to an increase in STOP1 protein levels.

transport chain is a significant source of ROS production (Moller et al. 2007). Physiological studies have shown that Al can induce H_2O_2 production in mitochondria by impairing mitochondrial function (Yamamoto et al. 2002; Huang et al. 2014; Zhan et al. 2014). Although H_2O_2 accumulation can be toxic to plant cells, it can also act as a signaling molecule to regulate plant stress responses (Castro et al. 2021; Mittler et al. 2022). However, it is currently unclear whether and how H_2O_2 plays a regulatory role in Al resistance.

Pentatricopeptide repeat (PPR) proteins are a group of modular proteins containing repeats of 35 amino acids; PRR protein is present in eukaryotes, with many more members in plants than other species (Schmitz-Linneweber and Small 2008; Barkan and Small 2014). The PPR family in plants can be divided into 2 subfamilies: P and PLS. P-type PPR proteins contain the canonical 35 amino-acid repeat (P) motif, while members of the PLS subfamily contain the P motif as well as longer (L) and short (S) variant PPR motifs (Fujii and Small 2011; Barkan and Small 2014). Most PPR proteins are located in mitochondria or chloroplasts, where they bind to 1 or several organellar transcripts to regulate their expression post-transcriptionally via RNA splicing, editing, cleavage, or translation (Barkan and Small 2014). Mutations in PPR genes that encode mitochondrion-localized PPR proteins frequently cause defects in embryo or seed development (Barkan and Small 2014), which can be attributed to an impairment of the mitochondrion electron transport chain.

Mitochondrial NADH-ubiquinone reductase (complex I), the major entry point of the electron transport chain, consists of 40 to 50 subunits, 9 of which are encoded by mitochondrial genes (Heazlewood et al. 2003; Sugiyama et al. 2005) that are frequently targeted by PPR proteins for promoting their RNA cleavage or editing (Yuan and Liu 2012; Zhu et al. 2012; Colas des Francs-Small et al. 2014; Leu et al. 2016; Wang et al. 2018; Yang et al. 2022). The Arabidopsis (*Arabidopsis thaliana*) genome encodes 450 PPR proteins, and different PPR members appear to show little functional redundancy (Barkan and Small 2014). Thus, many PPR proteins localizing to mitochondria remain to be identified and characterized. While some mutants in individual PPR genes have been reported to display defective responses to different stresses (Liu et al. 2010; Yuan and Liu 2012; Zsigmond et al. 2012; Zhu et al. 2014; Yang et al. 2022), the involvement of PPR proteins in Al resistance is currently unknown.

SENSITIVE TO PROTON RHIZOTOXICITY 1 (STOP1) is a C2H2-type zinc finger transcription factor that plays an essential role in regulating Al resistance and low pH tolerance (Iuchi et al. 2007). Recently, STOP1 has been demonstrated to be the master regulator for tolerance to a variety of other stresses, including low levels of phosphate, potassium, and oxygen (Balzergue et al. 2017; Mora-Macias et al. 2017; Enomoto et al. 2019; Wang et al. 2022), as well as salt and excess ammonium (Sadhukhan et al. 2019; Sadhukhan et al. 2021; Tian et al. 2021). STOP1 primarily regulates Al resistance by inducing the expression of *ALUMINUM-ACTIVATED MALATE TRANSPORTER 1* (*ALMT1*), whose encoding transporter mediates malate secretion (Iuchi et al. 2007), although the increased expression of other STOP1 target genes, including *MULTI-DRUG AND TOXIC COMPOUND EXTRUSION* (*MATE*), *ALUMINUM SENSITIVE 3* (*ALS3*), and *GLUTAMATE DEHYDROGENASE 1* (*GDH1*) and *GDH2*, also contributes to

Al resistance (Liu et al. 2009; Sawaki et al. 2009; Tokizawa et al. 2021). Recent research has shown that STOP1 is the subject of multiple layers of post-transcriptional regulation, including ubiquitination, SUMOylation, and phosphorylation (Zhang et al. 2019; Fang et al. 2020, 2021a, 2021b; Xu et al. 2021; Zhou et al. 2023); in addition, nucleocytoplasmic export of *STOP1* mRNA is under regulation (Guo et al. 2020). Al stress can trigger the MITOGEN-ACTIVATED PROTEIN KINASE KINASE KINASE 1 (MEKK1)–MITOGEN-ACTIVATED PROTEIN KINASE KINASE 1/2 (MKK1/2)–MITOGEN-ACTIVATED PROTEIN KINASE 4 (MPK4) cascade, which phosphorylates STOP1 (Zhou et al. 2023). Phosphorylation of STOP1 prevents its interaction with the F-box protein REGULATION OF ALMT1 EXPRESSION (RAE1), which mediates STOP1 ubiquitination and degradation, leading to an increase in STOP1 accumulation. H_2O_2 can mediate oxidative modification of proteins, including transcription factors, to alter their activity or stability (Peleg-Grossman et al. 2010; Marinho et al. 2014; Tian et al. 2018). It is unclear whether STOP1 is also subjected to H_2O_2-mediated oxidative modification to regulate its function.

In this study, we identified the mitochondrion-localized PPR protein RAE6 involved in modulation of mitochondrial *nad5* splicing. We show that mutation of *RAE6* impairs complex I activity of the mitochondrion electron transport chain and consequently induces H_2O_2 accumulation. Increased H_2O_2 accumulation promotes STOP1 oxidation, leading to RAE1-mediated STOP1 degradation, ultimately resulting in increased Al sensitivity. Conversely, decreasing H_2O_2 content or blocking STOP1 oxidation increased STOP1 stability and Al resistance. Our results demonstrate the important role of H_2O_2 in regulating Al resistance and STOP1 stability.

Results

Identification of *rae6* with lower STOP1 accumulation and Al resistance

We previously conducted a forward genetic screen on an ethyl methanesulfonate-mutagenized population in the *proALMT1:LUC* background, harboring the *ALMT1* promoter driving the firefly luciferase (*LUC*) reporter gene. From this screen, we identified a series of *rae* (regulation of *ALMT1* expression) mutants with altered LUC activity (Zhang et al. 2019), including the *rae6* mutant with decreased LUC signal (Fig. 1A). A reverse transcription quantitative PCR (RT-qPCR) analysis showed that the expression of *ALMT1*, *MATE*, and *ALS3*, which are regulated by STOP1 (Iuchi et al. 2007; Liu et al. 2009; Sawaki et al. 2009), is lower in *rae6* than in the wild-type (WT) control especially under +Al conditions (Fig. 1B). By contrast, the genes *SENSITIVE TO AL RHIZOTOXICITY 1* (*STAR1*), *ALS1*, and *STOP1*, which are not regulated by STOP1, were expressed at a similar level in the WT and the *rae6* mutant (Supplemental Fig. S1A), suggesting that mutation of *RAE6* impairs STOP1 function.

To investigate whether STOP1 protein accumulation is affected in *rae6* mutant, we crossed *proSTOP1:STOP1-GUS* (encoding a fusion between STOP1 and the β- glucuronidase [GUS] reporter) and *proSTOP1:STOP1-HA* transgenic lines, which were produced previously (Zhang et al. 2019), to the *rae6* mutant to introduce these transgenes into the mutant background. GUS staining and immunoblot analyses revealed that the STOP1-GUS and STOP1-HA protein levels are lower in the *rae6* background compared to WT under both −Al and +Al conditions (Fig. 1, C and D). To examine whether mutation of *RAE6* altered STOP1 stability, we treated roots with cycloheximide (CHX), a protein biosynthesis inhibitor, and exposed these roots to Al stress over time. An immunoblot analysis showed that STOP1-HA abundance decreases faster in *rae6* than in WT (Fig. 1E), indicating that the *rae6* mutation diminishes STOP1 stability.

Because of the lower expression of *ALMT1* in *rae6*, we compared the level of malate secretion in WT and the mutant: We determined that the mutant secretes less malate than the WT under both −Al and +Al conditions (Fig. 1F). We then determined the Al resistance phenotype of *rae6* by exposing seedlings of the WT, the *rae6*, and the Al-sensitive mutant control *hyper recombination1* (*hpr1*, also named *rae3*) (Guo et al. 2020) to different Al concentrations. Under control (−Al) conditions, the root length of *rae6* seedlings was similar to that of WT (Fig. 1G). However, under Al stress conditions, the relative root length of *rae6* and *hpr1* was much shorter than that of WT (Fig. 1G), indicating that *rae6* seedlings are more sensitive to Al than the WT. In agreement with these results, the *rae6* and *hpr1* mutants accumulated more Al than the WT in response to Al treatment (Fig. 1H). These data demonstrate that the *rae6* mutant decreases malate secretion and Al resistance.

In addition, the mutation of *RAE6* also adversely affected plant development. The *rae6* mutant displayed delayed flowering, shorter stature, and shorter siliques (Supplemental Fig. S1, B to D).

RAE6 encodes a mitochondrial-localized P-type PPR protein

We conducted a genetic analysis of *rae6* using a segregating F_2 population derived from a cross between *rae6* and Col-0. Among a total of 392 F_2 seedlings, 89 and 303 plants showed decreased and WT-like LUC signals, respectively. The ratio of the number of plants with a decreased LUC signal over the number of plants with a WT-like LUC signal fitted a 1:3 ratio ($\chi^2 = 1.1$, $P > 0.25$), suggesting that the decreased LUC signal in *rae6* is caused by a single recessive mutation.

To clone the *RAE6* gene, we pooled genomic DNA from the 89 F_2 plants with decreased LUC signal for whole-genome sequencing. We used the genomic sequence from the WT as control, which was sequenced previously (Zhang et al. 2019). We located the candidate mutation to a small region of chromosome 1 through MutMap analysis (Abe et al. 2012) (Supplemental Fig. S2). To verify the results of the MutMap analysis, we developed 5 derived cleaved amplified polymorphic sequence (dCAPS) markers within the candidate region based on the detected mutations in *rae6* relative to the

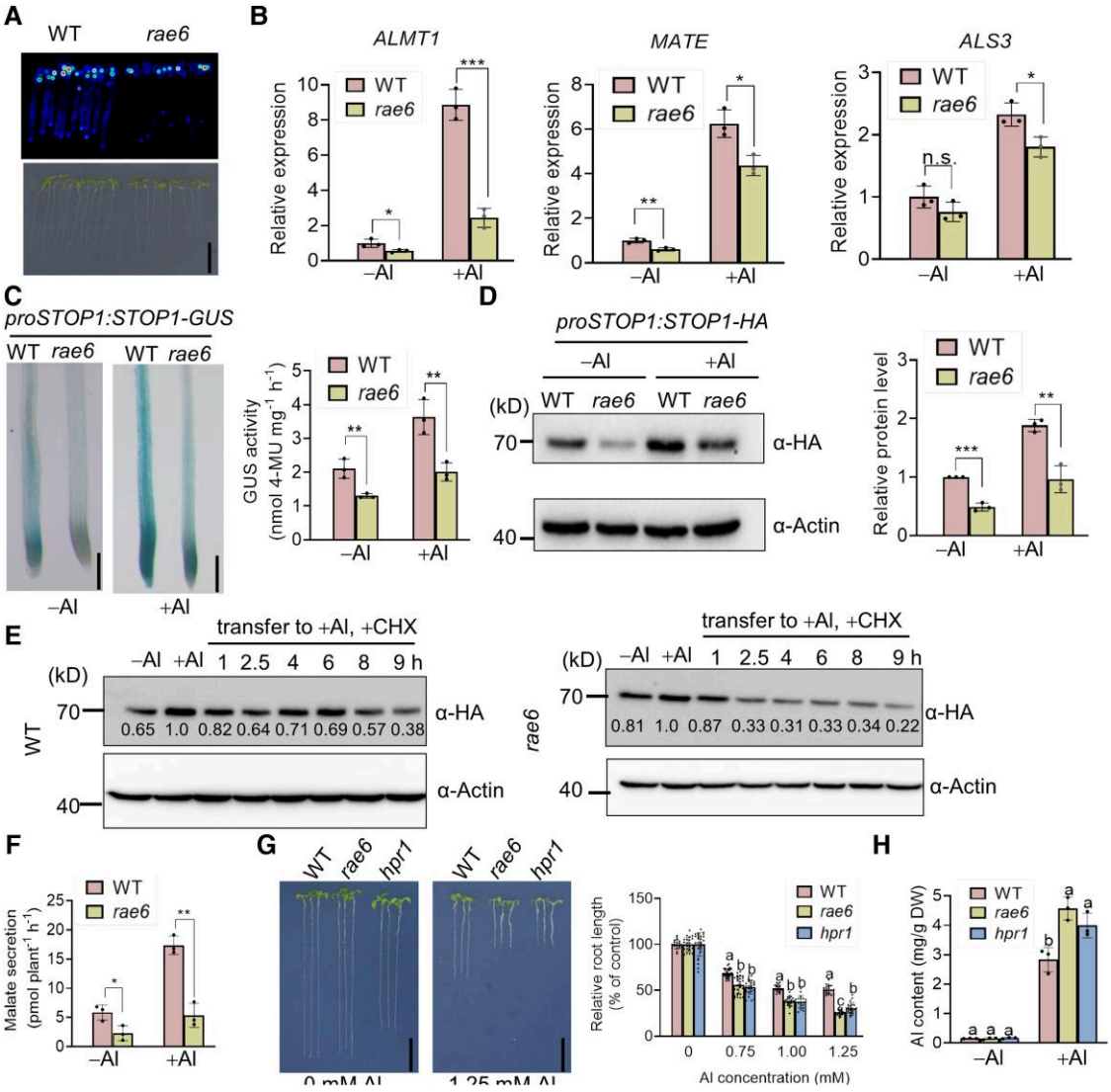

Figure 1. Mutation of *RAE6* decreases the expression of STOP1-regulated genes, STOP1 stability, and Al resistance. **A)** Decreased LUC signal of *proALMT1:LUC* in the *rae6* mutant. Scale bar, 1 cm. **B)** Lower expression of *ALMT1*, *MATE*, and *ALS3* in the *rae6* mutant. Seedlings of wild type (WT, Col-0) and *rae6* were cultivated on gel medium soaked with no (−Al) or 0.75 mM Al (+Al) for 7 d and then the roots were collected for RT-qPCR analysis. **C)** Representative photographs (left panel) and quantitative data (right panel) of GUS levels in roots of WT and *rae6* seedlings carrying the *proSTOP1:STOP1-GUS* transgene exposed to a 0.5 mM $CaCl_2$ solution containing no (−Al) or 30 μM Al (+Al) for 8 h. Scale bars, 200 μm. **D)** Representative immunoblot (left panel) and quantitative data (right panel) of STOP1-HA levels. WT and *rae6* seedlings carrying the *proSTOP1:STOP1-HA* transgene were grown on soaked gel medium containing no (−Al) or 0.75 mM Al (+Al) for 7 d; the roots were then collected for immunoblot analysis. Actin served as a loading control. **E)** Decreased STOP1 stability in *rae6*. The roots of WT and *rae6* seedlings harboring the *proSTOP1:STOP1-3HA* transgene were treated with 30 μM Al and/or 100 μM cycloheximide (CHX) alone for varying time intervals as indicated. **F)** Decreased malate release in *rae6*. WT and *rae6* seedlings were treated with a 0.5 mM $CaCl_2$ solution containing no Al or 20 μM Al for 12 h; the root exudates were analyzed for malate concentrations (pmol $plant^{-1}$ h^{-1}). **G)** Representative photographs (left panel) and quantitative data (right panel) of Al resistance in WT, *rae6*, and *hpr1*. Seedlings were grown on gel medium soaked with no Al or 0.75, 1, or 1.25 mM Al for 7 d; root relative length was measured to evaluate Al resistance. Scale bars, 1 cm. **H)** *rae6* accumulates more Al than WT in response to Al treatment. WT, *rae6*, and *hpr1* seedlings were exposed to a 0.5 mM $CaCl_2$ solution containing no Al or 20 μM Al for 12 h and then the Al content in the roots was determined. Data shown in **B to D)**, **F)**, and **H)** are means ± SD of 3 biological replicates; data shown in **G)** are means ± SD of the relative root length from 19 to 34 seedlings. Asterisks indicate statistically different values (Student's *t* test, $^*P < 0.05$, $^{**}P < 0.01$, $^{***}P < 0.001$). n.s., not significantly different. Different lowercase letters indicate significantly different means ($P < 0.05$, ANOVA followed by Tukey test).

WT sequence (Supplemental Table S1) and used the 89 F_2 plants to perform a marker linkage analysis. All 5 markers exhibited linkage to the mutant phenotype albeit to different extents, confirming that the *RAE6* gene is located in this region. We mapped *RAE6* between markers A1 and A3 with 5 and 3 remaining recombinants, respectively; notably, the A2 marker, based on a C-to-T substitution at the 1,981 bp position downstream from the start codon of

At1g73710, showed complete linkage to the mutant phenotype (Supplemental Table S1). This C-to-T substitution results in an amino acid change from leucine to phenylalanine (L661F) in At1g73710 in the *rae6* mutant. These results suggest that the L661F mutation in the protein encoded by At1g73710 may be responsible for the lower LUC signal and Al resistance observed in *rae6*.

To confirm that At1g73710 is *RAE6*, we attempted to construct a *proAt1g73710:At1g73710* transgene for complementation of *rae6*. However, we were unable to clone the At1g73710 DNA into a plasmid, which might be attributed to the complex secondary structure of At1g73710 DNA and/or the toxicity of At1g73710 when present in bacteria. As an alternative, we used an adenine base editor (A-to-G) (Wei et al. 2021) to convert the T-to-C mutation detected in At1g73710 in *rae6* back to the wild-type sequence of At1g73710. We obtained 1 plant (*rae6*^{F661L}) with the intended phenylalanine to leucine change (F661L) in At1g73710 in the *rae6* background from a screen of ∼120 transgenic plants. An RT-qPCR analysis showed that the decreased expression of STOP1-regulated genes in *rae6* returns to wild-type levels in *rae6*^{F661L} (Supplemental Fig. S3A). The lower Al resistance phenotype of *rae6* was also rescued in *rae6*^{F661L} (Supplemental Fig. S3B). In addition, we ordered 1 T-DNA line (GK-375A05-017161) with a T-DNA insertion in At1g73710 (Supplemental Fig. S4A). However, we were unable to obtain homozygous mutant plants. Observation of seeds from a selfed heterozygous plant showed that 81 out of 316 seeds are aborted (Supplemental Fig. S4B), suggesting that the knockout of At1g73710 leads to embryo death. We further knocked down the transcript levels of At1g73710 via RNA interference (RNAi) (Supplemental Fig. S4C) to determine its function. Similar to *rae6*, the expression of STOP1-regulated genes and Al resistance were also lower in 2 At1g73710 RNAi lines compared to WT (Supplemental Fig. S4, C and D). Together, these results indicate that *RAE6* is At1g73710, whose mutation causes a decrease in the expression of STOP1 target genes and Al resistance.

RAE6 encodes a P-type PPR family protein harboring 20 PPR motifs (Supplemental Fig. S4A). RT-qPCR analysis showed that *RAE6* is expressed at similar levels in all tissues examined (Supplemental Fig. S5A), and Al stress and the *rae6* mutation did not affect *RAE6* expression (Supplemental Fig. S5B). To determine the tissue-specific expression pattern of *RAE6*, we constructed *proRAE6:GUS* transgenic lines by driving the *GUS* reporter gene with the *RAE6* promoter. GUS staining analysis detected a GUS signal preferentially in root tips (Supplemental Fig. S5C). In shoots, we detected GUS staining in leaf vascular tissues and pollen (Supplemental Fig. S5C).

To investigate the subcellular localization of RAE6, we amplified a fusion construct consisting of *proUBQ10:RAE6-GFP* (encoding a fusion between RAE6 and the green fluorescent protein) and introduced the resulting PCR product into Arabidopsis protoplasts via transfection, since we could not clone *RAE6* in a bacterial vector, as mentioned earlier. While we observed GFP fluorescence in both the cytoplasm and nucleus in protoplasts transfected with *35S:GFP*, we determined that RAE6-GFP co-localizes with mitochondria, labeling with the fluorescent dye Mito Tracker (Fig. 2A), suggesting that RAE6 is localized to mitochondria.

Mutation of *RAE6* impairs the mitochondrial electron transport chain and induces H_2O_2 accumulation

A major function for P-type PPR proteins in chloroplasts and mitochondria is proposed to be the stabilization or splicing of specific organelle RNAs (Barkan and Small 2014). Given that RAE6 is localized to mitochondria (Fig. 2A), we compared the expression levels of 25 mitochondrial genes carrying no introns in WT and *rae6* by RT-qPCR, which revealed that the transcript levels of these genes are similar between WT and *rae6* (Supplemental Fig. S6A). We then compared the levels of full-length mature transcripts for 9 mitochondrial genes containing introns by end-point RT-PCR. We determined that the levels of full-length mature *nad5* transcripts are markedly lower in *rae6* compared to WT (Fig. 2B), whereas the levels of other transcripts did not show a significant difference between WT and the mutant (Supplemental Fig. S6B). To investigate whether the *rae6* mutation affected the splicing of *nad5* pre-RNA transcripts, which consists of 2 cis-spliced introns and 2 trans-spliced introns (Fig. 2C), we examined the splicing efficiencies of the 4 *nad5* introns in WT and *rae6*: We established that their splicing efficiencies are all lower in *rae6* compared to WT (Fig. 2D). The lower accumulation of mature *nad5* transcript and the defective splicing of *nad5* in *rae6* was rescued to WT levels in the *rae6*^{F661L} line (Fig. 2, B and D).

Since *nad5* encodes a subunit of mitochondrial complex I (NADH-ubiquinone oxidoreductase), we analyzed the accumulation of complex I in mitochondrial membrane proteins by blue native (BN)-PAGE: The abundance of complex I was decreased in *rae6* compared to WT (Fig. 2E). In concert with the lower accumulation of complex I in the mutant, *rae6* showed a decreased activity of complex I in comparison to the WT (Fig. 2F); these 2 phenotypes were again rescued back to WT levels in the *rae6*^{F661L} line (Fig. 2, E and F). Together, these results demonstrate that mutation of *RAE6* decreases the abundance and activity of mitochondrial complex I, likely through impairing *nad5* splicing.

Complex I is a major ROS production site in mitochondria; decreasing its function has been shown to induce ROS accumulation (Moller 2001; Yang et al. 2022). We thus compared ROS accumulation in WT and *rae6* under −Al and +Al conditions by using the ROS fluorescent probe 2′,7′-dichlorofluorescin diacetate (H_2DCFDA): We observed an induction of ROS accumulation under Al stress in the WT and in the *rae6* mutant regardless of Al stress, although treatment with Al further increased ROS accumulation (Fig. 3A). We further investigated where ROS accumulate by analyzing the co-localization of the ROS fluorescent probe with the mitochondria-labeling

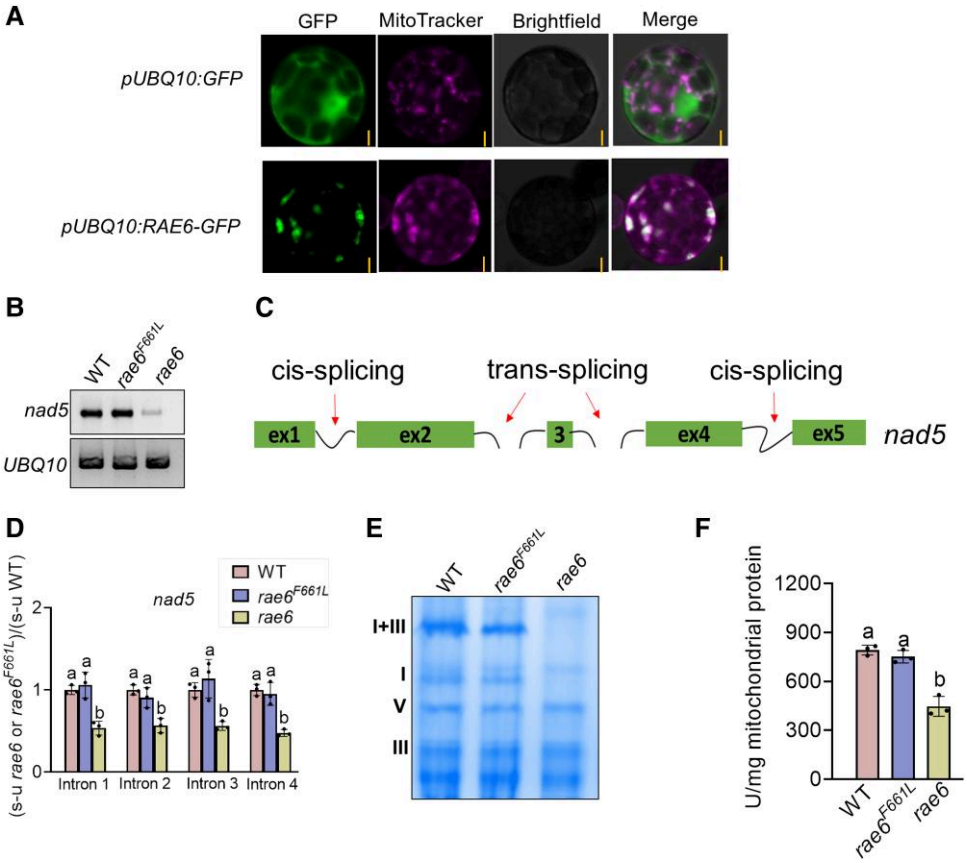

Figure 2. Subcellular localization of RAE6 and effect of the *rae6* mutation on *nad5* splicing and mitochondrial complex I accumulation. **A)** RAE6-GFP co-localizes with the mitochondrion fluorescent dye Mito Tracker in Arabidopsis protoplasts. Scale bars, 5 μm. **B)** RT-PCR analysis showing that the level of full-length *nad5* transcript is lower in *rae6* than in WT but returned to WT levels in *rae6*^{F661L}. **C, D)** Splicing diagram **C)** and splicing efficiency **D)** of *nad5* transcripts in WT, *rae6*^{F661L}, and *rae6*. RT-qPCR analysis was carried out to calculate the relative proportions of spliced (s) to unspliced (u) forms of *nad5* introns. **E)** Blue native PAGE gel analysis of the different mitochondrial respiratory complexes in WT, *rae6*^{F661L}, and *rae6*. **F)** Mutation of *RAE6* decreases mitochondrial complex I activity in roots. Data shown in **D)** and **F)** are means ± SD of 3 biological replicates. Different lowercase letters indicate significantly different means ($P < 0.05$, ANOVA test followed by Tukey test).

fluorescent dye Mito Tracker. We observed the accumulation of ROS within mitochondria following Al stress and in the *rae6* mutant (Fig. 3B). To examine the specific types of ROS being accumulated, we stained roots for superoxide and H_2O_2 using nitroblue tetrazolium (NBT) and 3,3′-diaminobenzidine (DAB), respectively. These staining assays demonstrated that the *rae6* mutant accumulates more H_2O_2 than WT, with Al stress also triggering H_2O_2 accumulation (Fig. 3C). However, we did not observe a significant difference in superoxide accumulation between WT and the mutant (Fig. 3D). Additionally, we measured the H_2O_2 production rate in isolated mitochondria and found that both Al stress and the *rae6* mutant increase the rate of mitochondrial H_2O_2 production (Fig. 3E). Consistent with the increased mitochondrial H_2O_2 production, the expression of *ALTERNATIVE OXIDASE* (*AOX*) genes, whose expression can be triggered by mitochondrial ROS (Maxwell et al. 1999; Vanlerberghe 2013), was induced significantly in the mutant compared to WT (Fig. 3F). These findings underscore the finding that Al stress and the *rae6* mutant can trigger mitochondrial H_2O_2 production.

Elevated H_2O_2 weakens Al resistance of *rae6* partly through limiting STOP1 accumulation

To investigate whether the increased H_2O_2 levels in *rae6* cause the observed lower Al resistance and STOP1 accumulation, we applied glutathione (GSH) to scavenge H_2O_2 and characterized the resulting Al resistance and expression of STOP1-regulated genes. The supply of GSH significantly rescued the Al-sensitive phenotype of *rae6*, as measured by relative root length, and partially rescued the decreased expression of STOP1-regulated genes in *rae6* (Supplemental Fig. S7, A and B). To corroborate this pharmacological result, we overexpressed *CATALASE 2* (*CAT2*) encoding a H_2O_2-scavenging enzyme in WT and *rae6* with or without a *proSTOP1:STOP1-HA* transgene. While overexpression of *CAT2* in WT slightly increased Al resistance to a high Al concentration, *CAT2* overexpression rescued the Al-sensitive phenotype of *rae6* at all Al concentrations tested (Fig. 4A). Immunoblot and expression analyses revealed that the lower abundance of STOP1-HA and the decreased expression of STOP1-regulated genes in *rae6* all return to WT levels upon the overexpression of *CAT2* (Fig. 4, B and C). We also introduced a mutant in

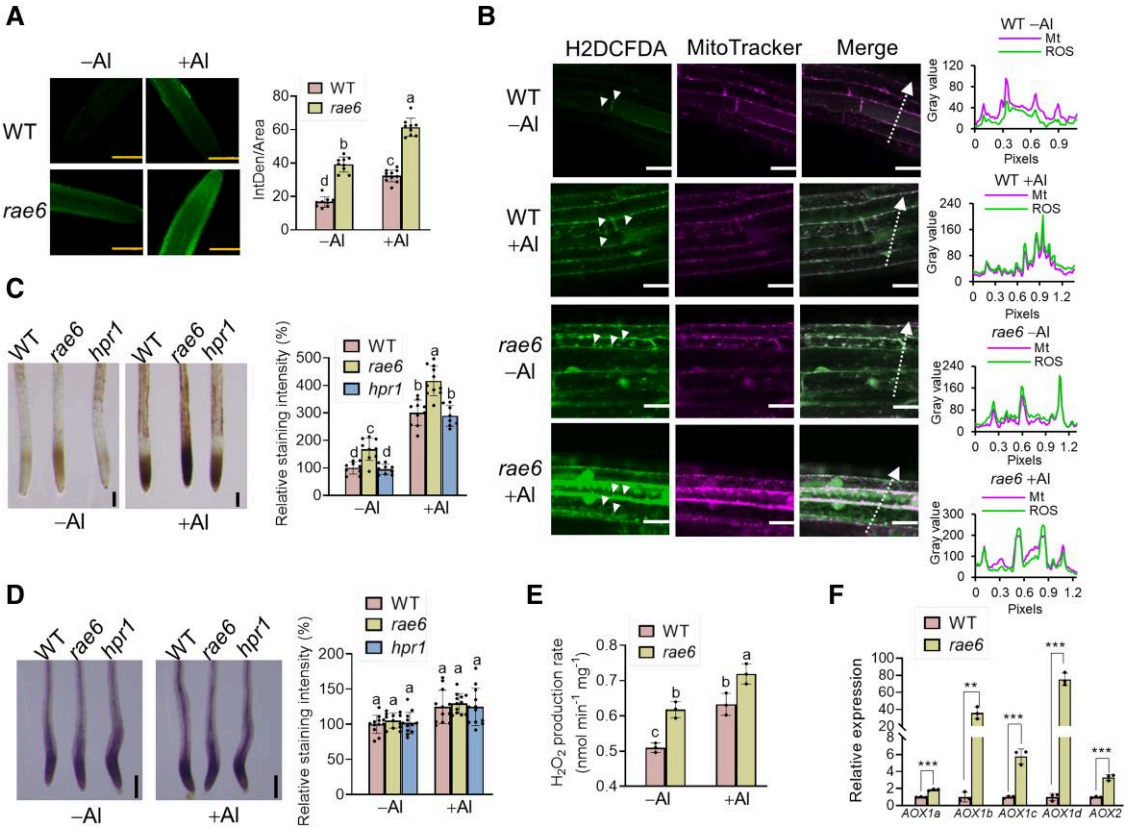

Figure 3. *Rae6* accumulates more H_2O_2 than WT. **A, B)** Effect of the *rae6* mutation on total ROS **A)** and mitochondrial ROS **B)** levels in the roots. Seven-day-old seedlings were transferred to soaked gel medium containing no Al or 0.75 mM Al for 12 h. ROS were visualized using the fluorescence probe H_2DCFDA, and mitochondria were stained using MitoTracker Red. White arrowheads indicate ROS accumulation in root mitochondria. Gray value plots on the right show the relative fluorescence along the dotted arrow line in the images. **C, D)** Effect of the *rae6* mutation on H_2O_2 **C)** and O_2^- **D)** accumulation. DAB and NBT were used to stain H_2O_2 and O_2^-, respectively. **E)** Effect of the *rae6* mutation and Al stress on rates of mitochondrial H_2O_2 production. The roots of 10-d-old seedlings treated with either no $AlCl_3$or 0.75 mM $AlCl_3$-soaked gel medium for 12 h were subjected to mitochondrial isolation. The rates of H_2O_2 production in isolated mitochondria were determined by fluorometric monitoring of Amplex Red conversion to resorufin. **F)** Increased expression of *AOX* genes in *rae6*. Scale bars in **A)**, **C)**, and **D)** represent 200 μm; or 20 μm in **B)**. Data shown are means ± SD of 3 biological replicates. Different lowercase letters indicate significantly different means ($P < 0.05$, ANOVA followed by Tukey test). Asterisks indicate statistically different values (Student's *t* test, $^{**}P < 0.01$, $^{***}P < 0.001$).

RESPIRATORY BURST OXIDASE HOMOLOG D (*RBOHD*) (Supplemental Fig. S8A), whose encoded protein is required for normal H_2O_2 production, into the *rae6* background through crossing. The *rbohD* mutant had a marked decrease in *RBOHD* expression (Supplemental Fig. S8B) and largely rescued the increased Al sensitivity, lower accumulation of STOP1-HA, and the diminished expression of STOP1-regulated genes seen in *rae6* when combined into the *rbohD rae6* double mutant (Supplemental Fig. S8, C to E). These results indicate that the increased H_2O_2 accumulation causes the Al-sensitive phenotype of *rae6* partially through decreasing STOP1 accumulation.

H_2O_2 induces STOP1 oxidation and negatively modulates STOP1 accumulation

H_2O_2 has well been documented to post-translationally regulate target proteins via cysteine oxidative modification (Moller et al. 2007; Tian et al. 2018; Lu et al. 2022). To examine whether H_2O_2 directly induces STOP1 oxidation, we treated recombinant STOP1-His with different concentrations of H_2O_2, followed by incubation with biotin-conjugated iodoacetamide (BIAM), which can compete with H_2O_2 to react with cysteine residues (Kim et al. 2000). An immunoblot analysis using an anti-biotin antibody showed that the abundance of biotin-labeled STOP1 decreases in the presence of H_2O_2 in a dose-dependent manner (Fig. 5A), suggesting that H_2O_2 promotes cysteine oxidation of STOP1. To determine whether STOP1 is oxidized in vivo, we extracted total proteins from the roots of WT and *rae6* seedlings harboring the *proSTOP1:STOP1-HA* transgene, after they were pretreated with H_2O_2 or Al. We employed a biotin-switch assay (Li and Kast 2017) to detect oxidized STOP1: Both H_2O_2 and Al were effective in triggering STOP1 oxidation, and mutation of *RAE6* increased STOP1 oxidation compared to WT under both normal and Al stress conditions (Fig. 5, B and C).

To determine which cysteine sites in STOP1 are oxidized by H_2O_2, we performed a liquid chromatography-tandem mass spectrometry analysis. Accordingly, we subjected

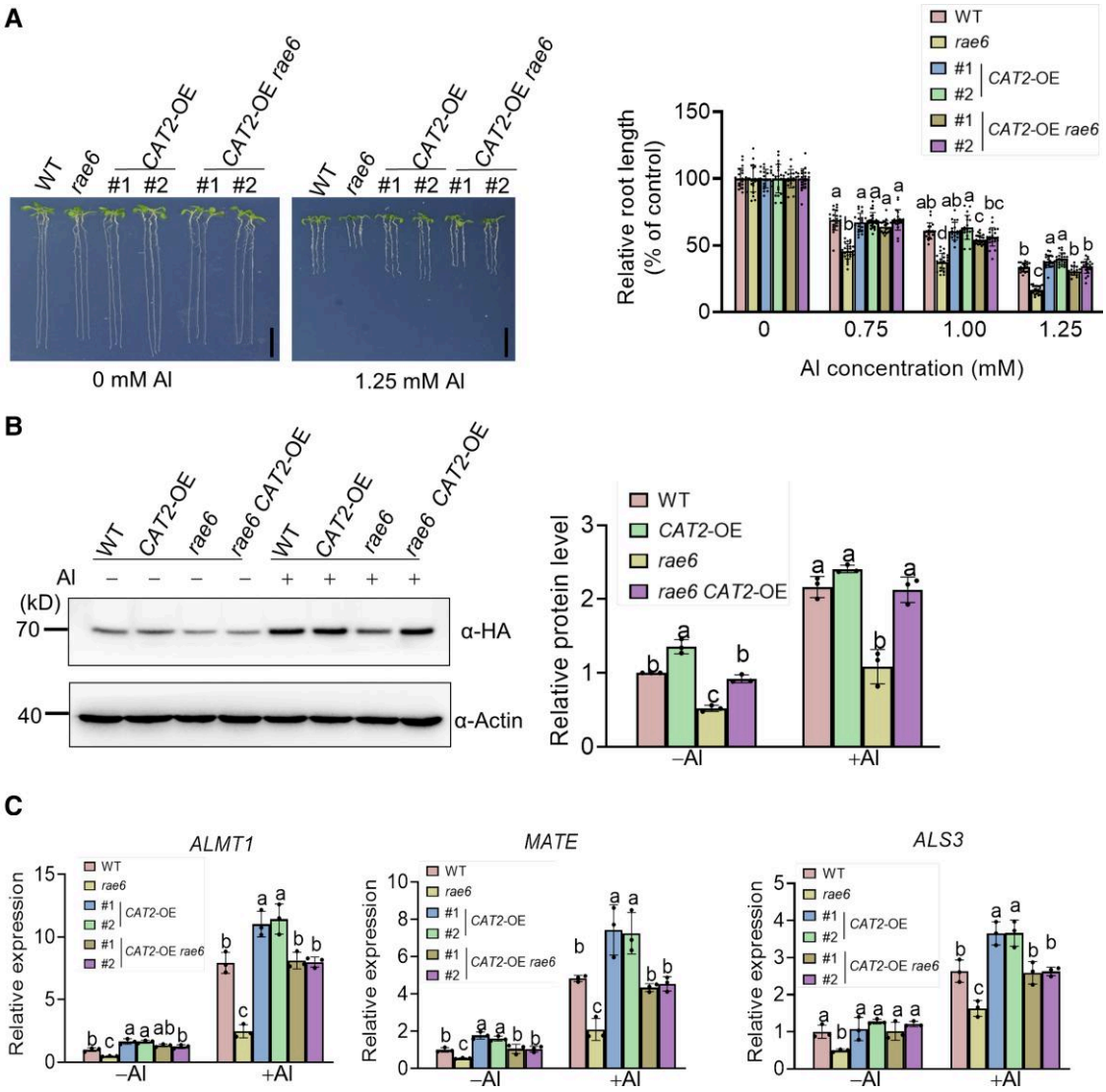

Figure 4. Overexpression of *CAT2* rescues the increased Al sensitivity and decreased STOP1 accumulation of *rae6*. **A)** Overexpression of *CAT2* rescues the Al-sensitive phenotype of *rae6*. Seedlings of WT, *rae6*, 2 *CAT2* overexpression lines (*CAT2*-OE), and 2 *CAT2*-OE in the *rae6* background were cultivated on gel medium soaked with no Al or 0.75, 1, or 1.25 mM Al for 7 d; root relative length was measured to evaluate Al resistance. Scale bars, 1 cm. Values are means ± SD (n = 18 to 27). **B, C)** Effect of *CAT2* overexpression on STOP1 accumulation **B)** and the expression of STOP1-regulated genes **C)**. Seedlings were grown on gel medium soaked with no Al or 0.75 mM Al for 7 d; the roots were collected for the determination of STOP1-HA accumulation and the expression of STOP1-regulated genes. Values are means ± SD of 3 biological replicates. Different lowercase letters indicate significantly different means ($P < 0.05$, ANOVA test followed by Tukey test).

recombinant STOP1-His to sequential treatment with H_2O_2, N-ethylmaleimide (NEM), and BIAM, followed by trypsin digestion. This analysis revealed that the cysteine residues Cys-8, Cys-27, and Cys-185 are oxidized residues in STOP1 (Supplemental Fig. S9). Subsequently, we replaced each cysteine by serine residues individually at the C8, C27, or C185 positions to investigate the major oxidized sites in STOP1. However, the single C-to-S mutations did not significantly decrease STOP1 oxidation (Fig. 5D). We thus generated the triple mutant C8S, C27S, C185S (3CS thereafter); remarkably, we established that H_2O_2-induced STOP1 oxidation is significantly diminished in this variant (Fig. 5D), suggesting that all 3 cysteine residues are necessary for STOP1 oxidation in vitro.

To explore whether these 3 cysteine residues are oxidized in vivo, we introduced the *proSTOP1:STOP1*^{3CS}*-3HA* (*STOP1*^{3CS}) construct into the *stop1* mutant background. We selected 2 *STOP1*^{3CS} lines with similar *STOP1* expression levels as the *proSTOP1:STOP1-3HA* (*STOP1*) complementation line (Supplemental Fig. S10). A biotin-switch assay demonstrated that oxidized STOP1 cannot be detected in the 2 *STOP1*^{3CS} lines, even in the presence of Al or H_2O_2, whereas we readily detected oxidized STOP1 in the *STOP1* line (Fig. 5, E and F). These results indicate that Al- or H_2O_2-induced

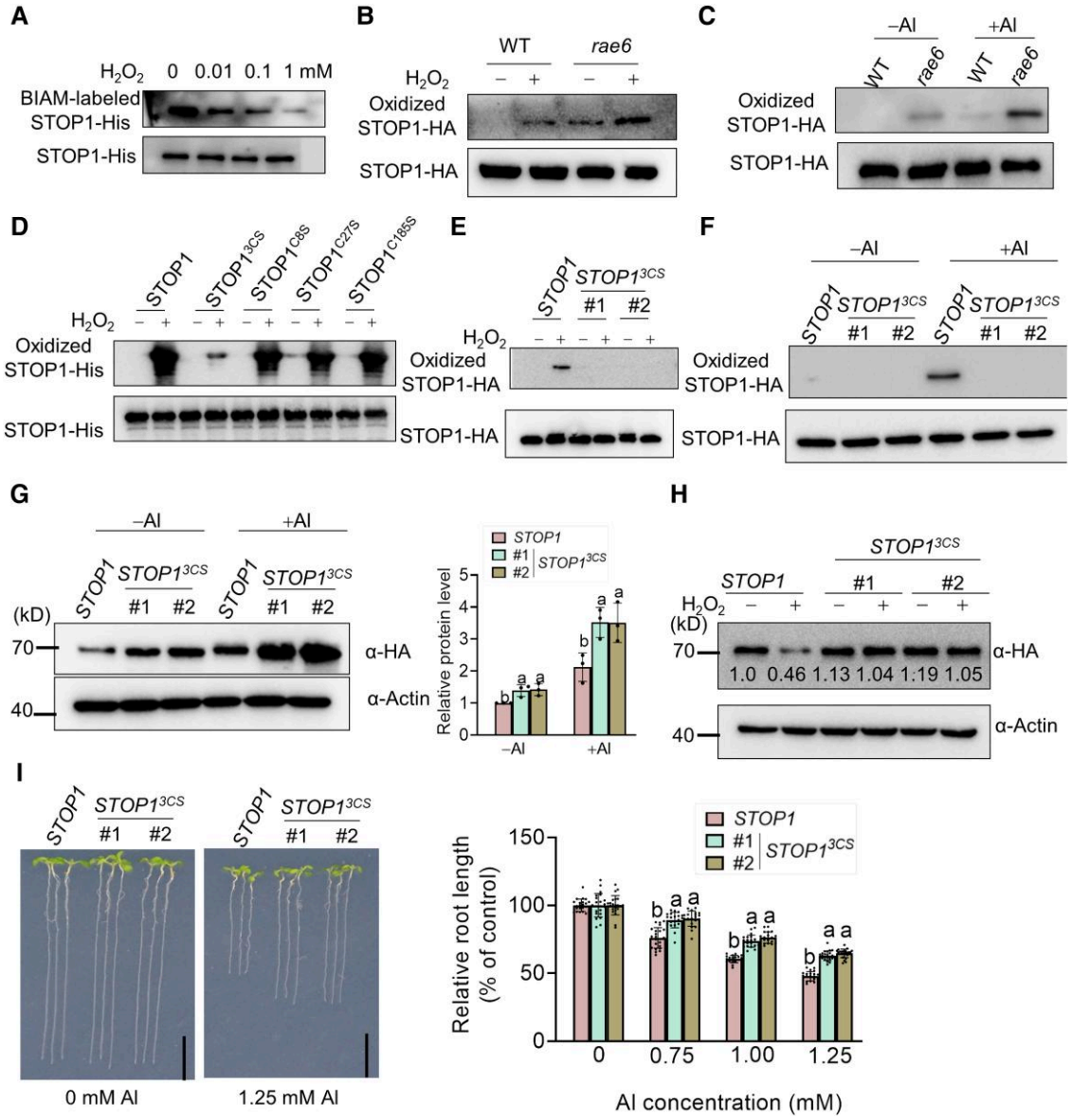

Figure 5. STOP1 is oxidized in vitro and in vivo. **A)** Analysis of the oxidative modification of STOP1 by a BIAM-labeling assay. **B)** Effect of H_2O_2 and the *rae6* mutation on STOP1 oxidation. Ten-day-old WT and *rae6* seedlings carrying the *proSTOP1:STOP1-HA* transgene were treated with no or 1 mM H_2O_2 for 3 h, and then the roots were collected for the determination of oxidized STOP1-HA through the biotin-switch assay. **C)** Effect of Al and the *rae6* mutation on STOP1 oxidation. WT and *rae6* seedlings carrying the *proSTOP1:STOP1-HA* transgene were grown on gel medium soaked with no Al or 0.75 mM Al for 7 d, and the biotin-switch assay was used to determine the oxidation state of STOP1-HA. **D)** Effect of single or triple C-to-S mutations at the C8, C27, and C185 residues of STOP1 on the oxidation of recombinant purified STOP1-His treated with no or 1 mM H_2O_2 for 15 min. **E to I)** Effect of triple C-to-S mutations (3CS) at the C8, C27, and C185 residues of STOP1 on H_2O_2- **E)** and Al- **F)** induced oxidation of STOP1, STOP1 accumulation **G)**, H_2O_2-induced degradation of STOP1 **H)**, and Al resistance **I)**. For H_2O_2 treatment, 9-d-old seedlings of *proSTOP1:STOP1-HA* and 2 *proSTOP1:STOP1^{3CS}-HA* (#1 and #2) transgenic lines in the *stop1* background were exposed to no or 1 mM H_2O_2 for 3 h. For Al treatment, seedlings were grown on gel medium soaked with no Al or 0.75 mM Al for 7 d. For Al resistance evaluation, seedlings were grown on gel medium soaked with no Al or 0.75, 1, or 1.25 mM Al for 7 d. Scale bars, 1 cm. Data shown in **G)** represent the means ± SD of 3 biological replicates; the data shown in **I)** represent the means ± SD (n = 20 to 24). Different lowercase letters indicate significantly different means ($P < 0.05$, ANOVA followed by Tukey test).

STOP1 oxidation specifically occurs at the C8, C27, and C185 residues in Arabidopsis.

To determine whether oxidation of STOP1 modulates its function, we compared the expression of STOP1-regulated genes in the *STOP1* and *STOP1^{3CS}* lines. We established that STOP1-regulated genes are expressed at higher levels in the *STOP1^{3CS}* lines than in the *STOP1* line (Supplemental Fig. S10A). In addition, the *STOP1^{3CS}* lines accumulated more STOP1 than the *STOP1* line (Fig. 5G). Moreover, H_2O_2 treatment rapidly promoted the degradation of

STOP1, but not of STOP1^{3CS} (Fig. 5H). Phenotypic analysis showed that the *STOP1*^{3CS} lines are more tolerant to Al stress than the *STOP1* line (Fig. 5I). Additionally, the introduction of the *STOP1*^{3CS} transgene into the *rae6* mutant background via crossing returned the Al-resistant phenotype of *rae6* back to WT level (Supplemental Fig. S10B). Taken together, these results suggest that Al stress triggers the oxidation of STOP1 at the C8, C27, and C185 residues, which negatively regulates STOP1 accumulation.

H_2O_2 promotes STOP1 degradation via enhancing its interaction with the F-box protein RAE1

To investigate whether H_2O_2 promotes STOP1 degradation via the 26S proteasome pathway, we treated the roots of WT and *rae6* seedlings carrying the *proSTOP1:STOP1-HA* transgene with MG132, an inhibitor of the 26S proteasome, or maintained them on normal growth medium as control. The lower STOP1 accumulation in *rae6* returned to WT levels after treatment with MG132 under both −Al and +Al conditions (Fig. 6A). The F-box protein RAE1 has been shown to play an important role in regulating STOP1 stability via the 26S proteasome pathway, with its homolog RAE1 HOMOLOG 1 (RAH1) also contributing to this regulation (Zhang et al. 2019; Fang et al. 2021b). We therefore generated a *rae1 rae6* double mutant alone or with the *proSTOP1:STOP1-HA* transgene by crossing. Phenotypic analysis revealed that the *rae1* mutation largely abolishes the increased Al sensitivity of *rae6* (Fig. 6B). Immunoblot and expression analyses showed that the lower accumulation of STOP1-HA and decreased expression of STOP1-regulated genes in *rae6* also return to WT levels in the *rae1 rae6* double mutant (Fig. 6C; Supplemental Fig. S11). These results suggest that H_2O_2 promotes the degradation of STOP1 via the RAE1/RAH1-mediated 26S proteasome pathway.

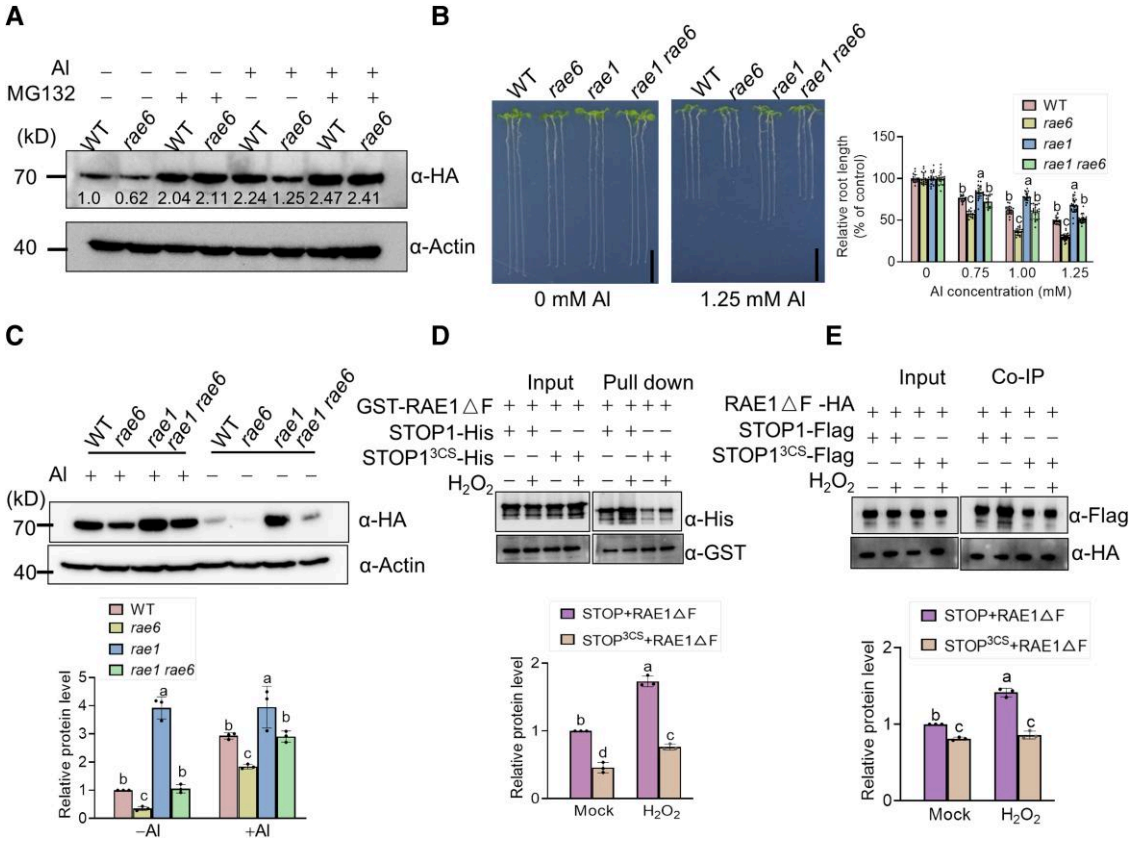

Figure 6. H_2O_2 promotes RAE1-mediated STOP1 degradation. **A)** Inhibition of *rae6* mutation-induced STOP1 degradation by MG132, an inhibitor of the 26S proteasome. **B)** Mutation of *RAE1* rescues the Al-sensitive phenotype of *rae6*. WT, *rae6*, *rae1*, and *rae1 rae6* seedlings were grown on gel medium soaked with no Al or 0.75, 1, or 1.25 mM Al for 7 d. Scale bars, 1 cm. **C)** Mutation of *RAE1* rescues the *rae6* mutation-induced degradation of STOP1. WT, *rae6*, *rae1*, and *rae1 rae6* seedlings carrying the *proSTOP1:STOP1-HA* transgene were grown on gel medium soaked with no Al or 0.75 mM Al for 7 d, and then the STOP1-HA level was determined by immunoblot analysis. **D, E)** Effect of H_2O_2 and triple C-to-S mutations (3CS) at the C8, C27, and C185 residues of STOP1 on the interaction between STOP1 and RAE1 lacking the F-box domain (RAE1ΔF) in pull-down **D)** and Co-IP **E)** assays. For the pull-down assay, recombinant GST-RAE1ΔF was incubated with STOP1-His or STOP1^{3CS}-His alone or with 1 mM H_2O_2 at 4 °C for 4 h. For the Co-IP assay, *RAE1ΔF-HA* was co-transfected with *STOP1-FLAG* or *STOP1*^{3CS}*-FLAG* in *rae1 rah1* protoplasts. Crude protein extracts were incubated with anti-HA magnetic beads alone or with 1 mM H_2O_2 at 4 °C for 4 h. Data shown in **B)** represent the means ± SD (n = 18 to 27); the data shown in **C to E)** represent the means ± SD of 3 biological replicates. Different lowercase letters indicate significantly different means ($P < 0.05$, ANOVA followed by Tukey test).

To investigate how H_2O_2 promotes the RAE1-mediated degradation of STOP1, we tested the interaction between STOP1-His or STOP1^{3CS}-His and a version of RAE1 lacking the F-box domain (RAE1ΔF) fused to glutathione S-transferase (GST) in a pull-down assay. We showed that RAE1ΔF has a stronger interaction with STOP1 than with STOP1^{3CS}, and H_2O_2 treatment promoted the interaction between RAE1ΔF and STOP1 (Fig. 6D). To confirm this observation, we performed a co-immunoprecipitation (Co-IP) assay in Arabidopsis protoplasts. Application of H_2O_2 also promoted the co-immunoprecipitation of RAE1ΔF-HA with STOP1-FLAG, and the association of RAE1ΔF-HA with STOP1-FLAG was stronger than with STOP1^{3CS}-FLAG (Fig. 6E). These results suggest that H_2O_2-induced STOP1 oxidation enhances the interaction between STOP1 and RAE1, resulting in STOP1 degradation.

The thioredoxin TRX1 catalyzes STOP1 reduction

To counteract the H_2O_2-mediated thiol oxidation of STOP1 cysteine residues, reducing systems are required to catalyze the conversion of STOP1 from its oxidized to its reduced form. The thioredoxin (TRX) system is thought to play an important role in cellular thiol-redox control in eukaryotes (Garcia-Santamarina et al. 2014). While most plant TRXs localize to chloroplasts or mitochondria, h-type TRXs typically localize in the cytoplasm or nucleus (Meyer et al. 2012). A previous study showed that the h-type thioredoxin TRX1 positively regulates Al resistance (Nakano et al. 2020), but the underlying Al resistance mechanism was unknown. We hypothesized that TRX1 might catalyze the reduction of STOP1 to confer Al resistance. Therefore, we investigated whether TRX1 can interact with STOP1. A pull-down assay indicated that GST-TRX1, but not GST alone, can form bind to STOP1-His (Fig. 7A), indicating that TRX1 can directly interact with STOP1 in vitro. To investigate whether TRX1 can interact with STOP1 in planta, we performed a split-LUC assay in the leaves of *Nicotiana benthamiana* plants. We detected a LUC signal only for the combination of *cLUC-TRX1* and *STOP1-nLUC* (Fig. 7B), reflecting the in planta interaction between TRX1 and STOP1. To investigate whether TRX1 and STOP1 formed a complex in Arabidopsis, we co-transfected Arabidopsis protoplasts with *TRX1-HA* or *GFP-HA* as control with *STOP1-FLAG* and performed a Co-IP. TRX1-HA, but not GFP-HA, was co-immunoprecipitated with STOP1-FLAG (Fig. 7C). To ascertain whether TRX1 indeed catalyzes the reduction of STOP1, we incubated recombinant STOP1 with H_2O_2 and/or TRX1, and then detected oxidized STOP1. We determined that TRX1 effectively decreases the H_2O_2-induced oxidation of STOP1 (Fig. 7D). Together, these findings show that TRX1 can interact directly with STOP1 to catalyze its reduction.

To investigate whether TRX1 can regulate STOP1 function, we used a previously reported knockout line for *TRX1* (Nakano et al. 2020). Expression analysis revealed that knockout of *TRX1* has no effect on *STOP1* expression (Supplemental Fig. S12A), but decreased the expression of STOP1-regulated genes under Al stress conditions (Supplemental Fig. S12A). We then introduced the *proSTOP1:STOP1-HA* transgene by crossing into the *trx1* background to investigate the effect of the *trx1* mutation on STOP1 accumulation. We observed that STOP1 abundance decreases in *trx1* compared to WT under Al stress conditions, but not under control conditions (Fig. 7E). Accordingly, *trx1* was more sensitive to Al than WT (Supplemental Fig. S12B), which is consistent with the previous report (Nakano et al. 2020). The lower expression of STOP1-regulated genes and Al-sensitive phenotype in *trx1* could be rescued in 2 *trx1* complementation lines (Supplemental Fig. S12, A and B). Furthermore, introduction of the *STOP1*^{3CS} transgene into the *trx1* mutant background by crossing also rescued the lower STOP1 abundance and Al-sensitive phenotype of *trx1* back to WT level (Supplemental Fig. S12, C and D). In addition, overexpression of *TRX1* completely rescued the decreased expression of STOP1-regulated genes and the Al-sensitive phenotype of *rae6* (Fig. 7, F and G). The biotin-switch assay detected a higher level of oxidized STOP1 in the *trx1* mutant and lower in the *TRX1* overexpression line than in the WT under Al stress conditions (Fig. 7H). Collectively, these findings suggest that TRX1 catalyzes STOP1 reduction to positively regulate STOP1 accumulation and Al resistance.

Discussion

H_2O_2 can be converted to the more reactive species OH•, which is toxic to cells, and it can also react with certain Cys residues of a protein to modulate its function (Garcia-Santamarina et al. 2014). Studies have shown that H_2O_2 is involved in the regulation of plant stress responses via oxidative post-translational modifications (oxi-PTMs) (Mittler et al. 2022). Nevertheless, it remains unknown whether H_2O_2 actively regulates Al resistance through oxi-PTMs. Our study shows that Al stress and/or the *rae6* mutant can induce H_2O_2 accumulation in roots, leading to the oxidation of STOP1 on its C8, C27, and C185 residues. This oxidation of STOP1 enhances its interaction with the F-box protein RAE1, thereby promoting STOP1 degradation, which in turn leads to decreased expression of STOP1-regulated genes and diminished Al resistance. To counteract the H_2O_2-mediated oxidation of STOP1, we also demonstrated that the thioredoxin TRX1 can interact with STOP1 to catalyze its reduction (Fig. 8).

We identified RAE6 as an uncharacterized, mitochondrion-localized P-type PPR protein using a forward genetic screen. P-type PPR proteins typically participate in splicing, cleavage, and translation of organellar transcripts, while PLS-type PPR proteins are generally involved in RNA editing (Barkan and Small 2014). Our findings support this notion by demonstrating that RAE6 participates in the splicing of mitochondrial *nad5* transcripts, which encode a subunit of mitochondrial complex I (Fig. 2). Maturation of the *nad5* transcript requires 2 cis- and 2 trans-splicing events to remove the 4 introns (Bonen 2008). While previous studies showed that 2 P-type PPR proteins, ORGANELLE TRANSCRIPT PROCESSING 439 (OTP439) and TANG2, are involved in removing *nad5* introns

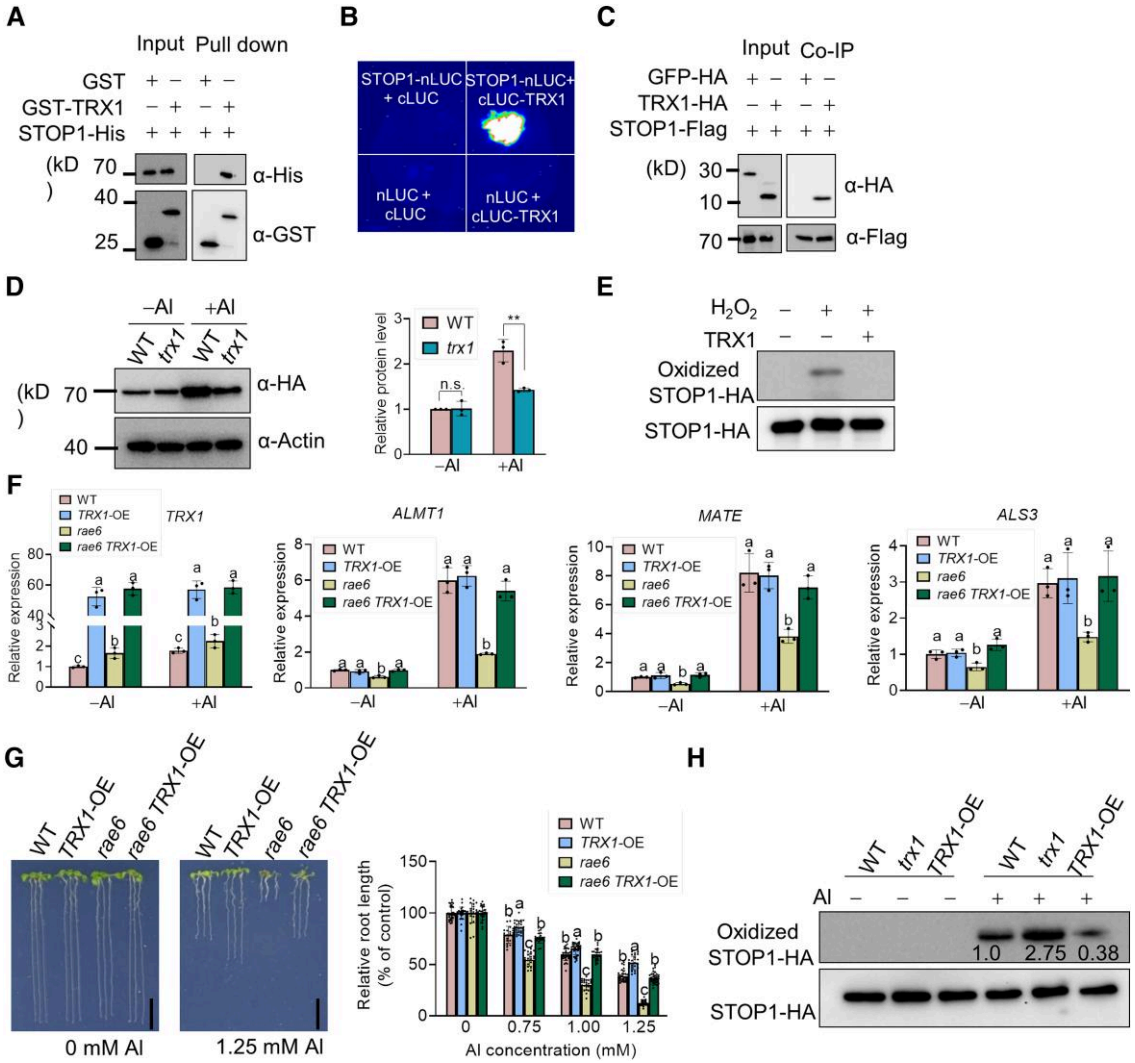

Figure 7. The thioredoxin TRX1 catalyzes STOP1 reduction. **A)** TRX1 directly interacts with STOP1 in vitro. Glutathione agarose beads containing GST or GST-TRX1 were incubated with STOP1-His. Bound proteins were detected by immunoblot analysis using anti-His and anti-GST antibodies. **B)** Split-LUC assay showing the interaction of STOP1 with TRX1. The indicated pairs of constructs were co-infiltrated in *N. benthamiana* leaves, and then luciferase activity was determined. **C)** Co-immunoprecipitation of TRX1 with STOP1. *STOP1-FLAG* was co-transfected with *TRX1-HA* or *GFP-HA* in Arabidopsis protoplasts. Crude protein extracts were immunoprecipitated with anti-FLAG magnetic beads and then probed with anti-HA antibody. **D)** TRX1 decreases the H_2O_2-induced oxidation of STOP1. Recombinant STOP1-His, pretreated with 1 mM H_2O_2, was incubated alone or with a TRX system comprising 0.5 mM NADPH, 1 μM TRX reductase, and 5 μg TRX1 for 3 h. Subsequently, oxidized STOP1 was detected using the biotin-switch assay. **E)** Mutation of *TRX1* decreases STOP1 accumulation. WT and *trx1* seedlings carrying the *proSTOP1:STOP1-HA* transgene were grown on gel medium soaked with no Al or 0.75 mM Al for 7 d; the roots were then collected for immunoblot analysis. **F)** Overexpression of *TRX1* rescues the decreased expression of STOP1-regulated genes in *rae6*. Seedlings of WT, *TRX1* overexpression line (*TRX1*-OE), *rae6*, and *rae6 TRX1*-OE were cultivated on gel medium soaked with no Al or 0.75 Al for 7 d; the roots were then collected for RT-qPCR analysis of *TRX1*, *ALMT1*, *MATE*, and *ALS3*. **G)** Overexpression of *TRX1* rescues the Al-sensitive phenotype of *rae6*. Seedlings were grown on gel medium soaked with no Al or 0.75, 1, or 1.25 mM Al for 7 d. Scale bars, 1 cm. **H)** Mutation and overexpression of *TRX1* increases and decreases the level of STOP1 oxidation, respectively. WT, *trx1*, and *TRX1*-OE seedlings carrying the *proSTOP1:STOP1-HA* transgene were grown on gel medium soaked with no Al or 0.75 mM Al for 7 d; the biotin-switch assay was used to determine the oxidation state of STOP1-HA. Data shown in **E)** and **F)** are means ± SD of 3 biological replicates; the data shown in **G)** represent the means ± SD (n = 20 to 35). Asterisks indicate statistically different values (Student's *t* test, $^{**}P < 0.01$). n.s., not significantly different. Different lowercase letters indicate significantly different means ($P < 0.05$, ANOVA followed by Tukey test).

2 and 3, respectively (Colas des Francs-Small et al. 2014), we showed here that RAE6 mediates splicing of all 4 introns of *nad5* (Fig. 2D). Due to defective splicing of *nad5*, the *rae6* mutant exhibited decreased mitochondrial complex I activity, resulting in defective mitochondrial electron transport chain (Fig. 2, E and F) and increased H_2O_2 accumulation (Fig. 3). Unlike the *rae6* mutant, which exhibited delayed flowering, shorter plant stature, and shorter siliques under normal

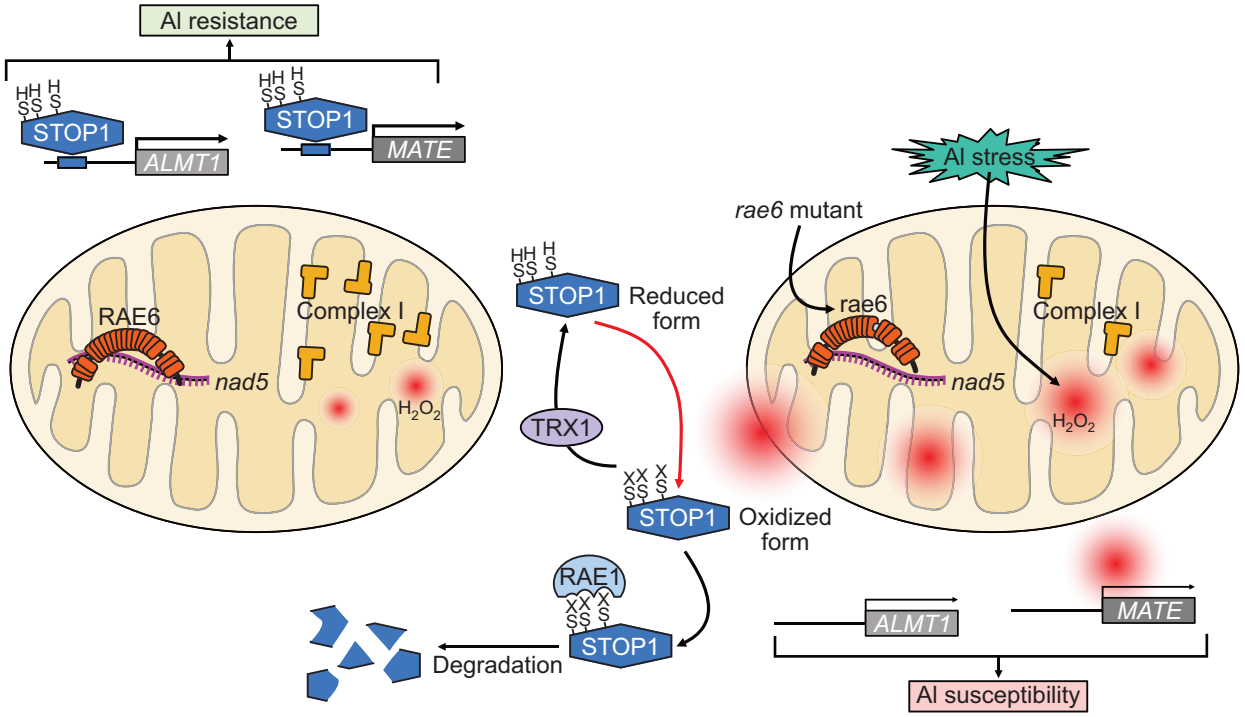

Figure 8. Model for regulation of STOP1 oxidation and stability. The PPR protein RAE6, localized in the mitochondrion, plays a crucial role in regulating the splicing of *nad5*, which encodes a component of mitochondrial complex I. Mutation of *RAE6* and/or exposure to Al stress result in the accumulation of mitochondrial H_2O_2. This H_2O_2 accumulation leads to the oxidation of STOP1 at the C8, C27, and C185 sites. Consequently, the interaction of STOP1 with the F-box protein RAE1 is enhanced, facilitating STOP1 degradation, which in turn leads to decreased expression of *ALMT1* and *MATE*, and ultimately causes reduced Al resistance. Additionally, the thioredoxin TRX1 interacts with STOP1 to catalyze its reduction.

growth conditions (Supplemental Fig. S1, B to D), knockout of *RAE6* results in seed abortion (Supplemental Fig. S4B). These findings suggest that RAE6 plays an essential role in plant development and that *rae6* is a weak mutant allele.

Several studies have revealed that Al stress can induce H_2O_2 accumulation in root mitochondria in pea and peanuts (*Arachis hypogaea*) (Yamamoto et al. 2002; Huang et al. 2014; Zhan et al. 2014). In the present study, we also show that Al can induce H_2O_2 production in Arabidopsis root mitochondria (Fig. 3, B and E). Our results indicate that Al-triggered H_2O_2 accumulation in mitochondria is not caused by modulation of *RAE6* expression or function, as Al stress did not affect *RAE6* expression (Supplemental Fig. S5B), and mitochondrial H_2O_2 production rate was similarly induced by Al in WT and *rae6* (Fig. 3E). Interestingly, we found that H_2O_2 induced by Al stress and in the *rae6* mutant is involved in the modulation of nucleus-localized STOP1 stability and Al resistance, suggesting that H_2O_2 plays a crucial role in Al signaling and plant response to Al stress. Since H_2O_2 has a relatively long half-life in living cells and can cross cell membranes and migrate to different compartments to exert its signaling functions (Bienert et al. 2006), we hypothesized that H_2O_2 directly mediates the oxidation of STOP1 to regulate its function. Our results support this hypothesis, as we determined that H_2O_2 can directly catalyze the oxidation of STOP1 at residues C8, C27, and C185 and promote the degradation of STOP1 (Supplemental Fig. S9; Fig. 5). Moreover, we showed that the total level of H_2O_2, rather than the source of H_2O_2, determines STOP1 oxidation, as both overexpression of *CAT2* encoding the peroxisomal H_2O_2-scavenging enzyme CATALASE2 and mutation of *ROBHD* encoding a plasma membrane-localized H_2O_2-producing oxidoreductase can rescue the lower accumulation of STOP1 and diminished Al resistance of *rae6* (Fig. 4; Supplemental Fig. S8).

As a crucial intracellular signaling molecule, H_2O_2 can mediate oxidation of redox-sensitive transcription factors, transmitting a ROS signal into the transcriptional regulatory network (Garcia-Santamarina et al. 2014; Schmidt and Schippers 2015). The oxidation of various transcription factors can have different functional effects. For instance, while H_2O_2-induced oxidation of NONEXPRESSER OF PR GENES 1 (NPR1), an essential regulator of plant systemic acquired resistance, inhibits its localization to the nucleus (Mou et al. 2003), oxidation of the basic leucine zipper (bZIP) transcription factor bZIP16 or the cold-responsive C-REPEAT-BINDING TRANSCRIPTION FACTORs (CBFs) inhibits their DNA binding activities (Shaikhali et al. 2012; Lee et al. 2021). Moreover, Tian et al. (2018) reported that H_2O_2-triggered oxidation of the transcription factor BRASSINAZOLE-RESISTANT 1 (BZR1), a master regulator of brassinosteroid signaling, enhances its transcriptional activity by promoting its interaction with other transcription factors, including AUXIN RESPONSE FACTOR 6 (ARF6) and PIF4. By contrast, our findings indicate that STOP1 oxidation induced by H_2O_2 enhances its interaction

with the F-box protein RAE1 and consequently promotes its degradation via the 26S proteasome pathway (Fig. 6).

The H_2O_2-mediated oxidation of thiol to disulfide in cysteine residues is reversible, primarily catalyzed by thioredoxins (TRXs) (Mittler et al. 2022). TRXs are thiol-disulfide oxidoreductases that reduce their target proteins by formation of an intermolecular mixed disulfide bond between the N-terminal cysteine of the CXXC motif of TRXs and their target proteins (Garcia-Santamarina et al. 2014; Mittler et al. 2022). Arabidopsis has various types of TRXs, among which only h-type TRXs are documented to mediate the reduction of transcription factors. For instance, TRX-h5 catalyzes the switch for BZR1 from its oxidized to its reduced form (Tian et al. 2018), while TRX-h2 reduces oxidized CBF oligomers to monomers (Lee et al. 2021). In this study, we demonstrated that the h-type TRX TRX1 directly interacts with STOP1 to catalyze its reduction (Fig. 7, A to D). Mutation of *TRX1* increases STOP1 oxidation induced by Al stress and subsequently decreases STOP1 accumulation (Fig. 7, E and H), while overexpression of *TRX1* counters *rae6*-induced STOP1 oxidation and degradation (Fig. 7, F and H). In a previous genome-wide association study, TRX1 was identified as an important locus explaining Al-tolerance variation in diverse Arabidopsis accessions (Nakano et al. 2020), suggesting that the selection of different *TRX1* alleles with different expression levels might help regulate the oxidation and accumulation levels of STOP1.

The degradation of STOP1 induced by H_2O_2 appears to be detrimental to plant resistance against Al stress. However, Al stress can activate the MEKK1–MKK1/2–MPK4 cascade, which phosphorylates and stabilizes STOP1 (Zhou et al. 2023). This phosphorylation may counteract the oxidation of STOP1, ultimately resulting in increased STOP1 accumulation in response to Al stress. While an increase in STOP1 levels can enhance Al resistance, it can also inhibit plant growth (Fang et al. 2021b). H_2O_2-induced degradation of STOP1 may allow plants to fine-tune the regulation of STOP1 levels, striking a balance between Al resistance and plant growth.

Materials and methods

Plant materials and growth conditions

All genotypes used in this study were in the Arabidopsis (*A. thaliana*) accession Columbia-0 (Col-0) background. The previously identified and described genotypes include *hpr1* (*rae3*), *rae1* (*rae1-1*), *proSTOP1:STOP1-GUS*, *stop1 proSTOP1:STOP1*^{C8S,C27S,C185S}*-3HA*, and *trx1* (Zhang et al. 2019; Guo et al. 2020; Nakano et al. 2020). The *rbohD* mutant (SALK_005253.55.50.x) was obtained from the Arabidopsis Biological Resource Center (ABRC).

Arabidopsis seeds were disinfected with 6% NaClO for 8 min and grown on solid half-strength Murashige and Skoog (MS) medium containing 1.2% (w/v) agar and 1% (w/v) sucrose for 7 d at 22 °C in a growth chamber (CU36L4, Percival). The seedlings were then examined for luciferase luminescence using a CCD imaging apparatus (Lumazone P1300B, Roper Scientific) or transferred to soil and grown at 22 °C under a photoperiod of 14 h of light (100 μmol/m^2/s, Philips TL-D 26W/865 cool daylight tubes) and 10 h of darkness. For split-LUC assays, *N. benthamiana* seeds were sown on soil and grown under the same conditions as Arabidopsis.

Measurement of malate secretion and Al content

To measure malate secretion, WT and *rae6* seeds were cultivated on 1.2% (w/v) agar medium containing half-strength MS medium and 1% (w/v) sucrose for 5 d. Seedlings were pretreated with a 2% (w/w) nutrient solution (Fujiwara et al. 1992), composed of 1.75 mM sodium phosphate buffer (pH 5.8), 1.5 mM $MgSO_4$, 2.0 mM $Ca(NO_3)_2$, 3.0 mM KNO_3, 67 μM Na_2EDTA, 8.6 μM $FeSO_4$, 10.3 μM $MnSO_4$, 30 μM H_3BO_3, 1.0 μM $ZnSO_4$, 24 nM $(NH_4)_6Mo_7O_{24}$, 130 nM $CoCl_2$, 1 μM $CuS0_4$, and 1% (w/v) sucrose, for 2 h at pH 4.8. Subsequently, the seedlings were treated with the same solution containing either no $AlCl_3$ or 10 μM $AlCl_3$ at pH 4.8 for 12 h in a 12-well plate with shaking. The root exudates were collected and concentrated using a freeze-dryer (Alpha 1-2 LDplus; Martin Christ Gefriertrocknungsanlagen GmbH, Osterode am Harz, Germany). The malate concentration in the root exudates was measured using the NAD^+/NADH enzymatic cycling method (Hampp et al. 1984).

To determine Al content in roots, 3-wk-old wild-type, *rae6*, and *hpr1* plants, grown in 1/10 Hoagland hydroponic solution, were pretreated with a 0.5 mM $CaCl_2$ solution for 6 h. Subsequently, the plants were treated with the same $CaCl_2$ solution alone or with 20 μM $AlCl_3$ for 12 h. Al content in the roots was determined using a recent method (Ligaba-Osena et al. 2017). Briefly, plant roots were immersed in a 0.5 mM citrate solution (pH 4.2) at 4 °C for 30 min to desorb Al bound in the apoplast and/or precipitated on the root surface. Afterward, the roots were rinsed 3 times with 18 MΩ water, gently blotted on paper towels, and carefully separated before transferred to preweighed test tubes. The tissues were then dried at 65 °C for 2 d, and their weights were measured. Subsequently, the tissues were digested with 2 mL of concentrated HNO_3 and diluted to a final volume of 10 mL with 2% HNO_3. The concentration of Al in the diluted solution was measured using inductively coupled plasma mass spectrometry (NexION300D; PerkinElmer, Waltham, Massachusetts, United States of America).

Evaluation of Al resistance

The method used to evaluate Al resistance was a modified version of the soaked gel medium method previously described (Larsen et al. 2005). The gel medium was prepared by combining the following components: 50 mL (pH 5.0) of 0.25 mM $(NH_4)_2SO_4$, 1 mM KNO_3, 0.2 mM KH_2PO_4, 2 mM $MgSO_4$, 1 mM $Ca(NO_3)_2$, 1 mM $CaSO_4$, 1 mM K_2SO_4, 1 mM $MnSO_4$, 5 mM H_3BO_3, 0.05 mM $CuSO_4$, 0.2 mM $ZnSO_4$, 0.02 mM $NaMoO_4$, 0.1 mM $CaCl_2$, 0.001 mM $CoCl_2$, 1% (w/v) sucrose, and 0.4% (w/v) Gellan gum (G1910; Sigma-Aldrich).

The medium was allowed to solidify, after which 35 mL (pH 3.6) of the same nutrient solution (without Gellan gum) containing no $AlCl_3$ or 0.75, 1.0, or 1.25 mM $AlCl_3$ was added to soak the medium. After 2 d of soaking, the remaining solution was removed, and seedlings were grown on the gel medium for 7 d. Subsequently, the seedlings were imaged, and root lengths were measured using ImageJ software. Relative root length, calculated as a percentage of root length with Al treatment relative to root length without Al (×100), was used to assess Al resistance.

Cloning of *RAE6*

To perform genetic analysis and mapping-by-sequencing, the *rae6* mutant was crossed to its wild type to construct an F_2 population. Eighty-nine F_2 plants exhibiting lower LUC signal from the *proALMT1:LUC* reporter were selected, and their genomic DNA was pooled for high-throughput DNA sequencing using an Illumina HiSeq4000 system, which was performed by a commercial company (Shanghai Hanyu Biotech Lab, Shanghai, China) (NCBI accession no. SRR9613722). The MutMap method (Abe et al. 2012) was employed to identify the candidate region for *rae6*. To validate the candidate region, a linkage analysis was conducted on the same 89 F_2 plants using 6 dCAPS markers. These markers were developed based on the single nucleotide polymorphisms between the wild type and *rae6* within the candidate region. Among the dCAPS markers employed, marker A2, which is based on a C-to-T substitution in At1g73710, exhibited complete linkage to the mutant phenotype (Supplemental Table S1). This result suggests that At1g73710 is *RAE6*.

To confirm the association between At1g73710 and *RAE6*, an adenine base editor (A-to-G) (Wei et al. 2021) was used to convert the T-to-C mutation in At1g73710 in *rae6* back to the wild-type sequence of At1g73710 by designing a 20 bp single guide RNA (sgRNA) targeting the mutation site (Supplemental Data Set 1). Among approximately 120 transgenic plants screened, 1 specific plant ($rae6^{F661L}$) was identified that carried the desired C-to-T mutation in At1g73710 within the *rae6* background. This plant or its progeny was used for expression analysis and phenotypic analysis related to aluminum resistance. Furthermore, to generate knockdown lines for At1g73710 using RNAi, a portion of the At1g73710 coding sequence (201 bp) was amplified with a specific primer pair (Supplemental Data Set 1) and cloned into the pANDA vector by GATEWAY (11791020, Invitrogen) cloning. Two transgenic lines with lower transcript levels of At1g73710 were obtained and subjected to the analysis and phenotypic analysis related to aluminum resistance.

RT-PCR analysis

To analyze the expression of Al resistance genes, seedlings were cultivated on gel medium soaked with no $AlCl_3$ or 0.75 mM $AlCl_3$ for 7 d. The roots of approximately 30 seedlings were excised for RNA isolation in each of 3 separate sets of seedlings. Total RNA was extracted from each sample using TRIzol reagent (Beyotime), and DNase I treatment (Vazyme Biotech, Nanjing, China) was performed to eliminate DNA contamination. Approximately 1 μg of total RNA was used for first-strand cDNA synthesis using a HiScript 1st Strand cDNA Synthesis Kit (Vazyme Biotech, Nanjing, China). qPCR analysis was conducted using 1/10 of the cDNA products in combination with 2×Universal SYBR Green Fast qPCR Mix (ABclonal, Wuhan, China) on a CFX96 Touch real-time PCR detection system (Bio-Rad). The reference gene was *UBQ10*.

To investigate the expression of mitochondrial genes, the roots of 9-d-old seedlings grown on half-strength MS agar medium were excised for RNA extraction. First-strand cDNA synthesis was performed using random hexamer primers. qPCR and end-point RT-PCR methods were employed to assess the expression of mitochondrial genes without or with introns, respectively. For the analysis of splicing efficiency in the 4 introns of *nad5*, specific primers were designed to target intron–exon junctions (unspliced forms) or exon–exon junctions (spliced forms). The primers used for the expression analysis can be found in Supplemental Data Set 1.

Mitochondrion isolation, BN-PAGE, and mitochondrial complex I activity assay

Mitochondrion isolation was conducted following the protocol outlined by Kelly and Wiskich (1988). In brief, approximately 10 g fresh roots of 12-d-old seedlings were ground and homogenized at 4 °C using a Mitochondrial Isolation Kit (P0045; Biohao, Wuhan, China). Following homogenization, the sample was centrifuged at 1,000 × *g* for 10 min at 4 °C to eliminate the nucleus and cell debris. Subsequently, the mitochondria were precipitated and collected by centrifuging the supernatant at 16,000 × *g* for 10 min at 4 °C. For BN-PAGE, the procedure was conducted following a previously described method (Colas des Francs-Small et al. 2014). In brief, 75 μg of mitochondrial protein was treated with 1% (w/v) dodecylmaltoside, and the native protein complexes were separated on a 5% to 13.5% (w/v) acrylamide gradient gel. The activity of complex I was assessed using a CheKine Micro Mitochondrial complex I Activity Assay Kit (KTB1850; Abbkine, California, United States of America). This kit detects the activity of the mitochondrial respiratory chain complex by measuring the oxidation rate of NADH at 340 nm. Complex I catalyzes NADH dehydrogenation to generate NAD^+, and the activity of the enzyme can be calculated directly by reading the oxidation rate of NADH at 340 nm.

Transient expression in protoplasts

Arabidopsis protoplasts were isolated from 14-d-old seedlings using a previously described method (Zhai et al. 2009). To investigate protein–protein interactions between STOP1 and TRX1, as well as between RAE1 lacking the F-box domain (RAE1ΔF) and intact of mutated STOP1, 2 mL of wild-type protoplasts (~2×10^6 cells/mL) was co-transfected with 50 μg of *35S:TRX1-2HA* and either 50 μg of

35S:STOP1-2FLAG or *35S:GFP-2FLAG* for the first experiment. For the second experiment, 2 mL of *rae1 rah1* protoplasts was co-transformed with 50 μg of *35S:RAE1ΔF-3HA* and either 50 μg of *35S:STOP1-2FLAG* or *35S:STOP1*^{C8S,C27S,C185S} (*STOP1*^{3CS})*-2FLAG*. Total proteins were extracted using 200 μL of protein extraction buffer containing 20 mM Tris-HCl (pH 7.5), 300 mM NaCl, 5 mM $MgCl_2$, 50 μM MG132 (A2585; APExBIO, United States of America), 0.5% (v/v) NP-40, and 1×Complete Protease inhibitor tablets EDTA-free (5892791001, Roche). An aliquot of 20 μL of the protein extract was saved as an input control. The remaining cell extracts were diluted to 1 mL alone or with 1 mM H_2O_2 and then incubated with 20 μL of anti-FLAG or anti-HA M2 magnetic beads for 4 h at 4 °C with gentle rotation. The protein-bound beads were washed 4 times with 1 mL of protein extraction buffer, and the bound proteins were eluted with 1×SDS loading buffer for immunoblot analysis using anti-FLAG-HRP, 1:5,000 (A8592; Sigma-Aldrich) or anti-HA-HRP, 1:2,000 (12013819001, lot 44323100, Roche) antibodies.

Subcellular localization analysis

To investigate the subcellular localization of RAE6, a 1.7 kb promoter fragment of *UBQ10*, the full-length *RAE6* coding sequence and *GFP* were separately amplified and then fused together using overlapping PCR (*proUBQ10:RAE6-GFP*). The PCR products of *proUBQ10:RAE6-GFP* were transfected into Arabidopsis mesophyll protoplasts, followed by cultivation in dark conditions for 16 h at 22 °C. Subsequently, the protoplasts were stained with 100 nM MitoTracker Red CMXRos for 20 min at 37 °C and observed using a confocal laser scanning microscope (ZEISS LSM880) to visualize the green and red fluorescence signals.

Pull-down assay

The coding sequences of *TRX1* or *RAE1ΔF* and *STOP1* or *STOP1*^{C8S,C27S,C185S} (*STOP1*^{3CS}) were individually cloned into the pGEX4T-1 and pET29a (+) vectors, respectively, resulting in the generation of *GST-TRX1*, *GST-RAE1ΔF*, *STOP1-His*, and *STOP1*^{3CS}*-His* recombinant plasmids. Each plasmid was then transformed into *Escherichia coli* strain BL21 (DE3) for production of the target proteins. The BL21 (DE3) cells were initially cultured at 37 °C to the OD600 at 0.6 and subsequently incubated at 16 °C for 16 h in the presence of 0.1 mM IPTG to induce protein production. For the TRX1 and STOP1 protein interaction assay, glutathione beads containing 20 μg of either GST or GST-TRX1 were incubated with 20 μg of STOP1-His at 4 °C for 4 h. In the protein interaction assay involving RAE1ΔF and STOP1 or STOP1^{C8S,C27S,C185S}, the glutathione beads containing 20 μg of GST-RAE1ΔF and either no or 1 mM H_2O_2 were incubated with 20 μg of STOP1-His or 20 μg of STOP1^{3CS}-His at 4 °C for 4 h. Following elution from the beads, the protein complexes were detected using immunoblotting with anti-GST or anti-His antibodies.

Split luciferase complementation (split-LUC) assays

The coding sequences of *STOP1* and *TRX1* were individually cloned into the pCAMBIA1-nLUC and pCAMBIA1-cLUC vectors, respectively. Subsequently, *STOP1-nLUC* was co-infiltrated with *cLUC-TRX1* into fully expanded *N. benthamiana* leaves via Agrobacterium-mediated infiltration. The infiltrated plants were then cultivated under long-day conditions for 2 d, and LUC signals from the infiltrated leaves were examined.

Detection of ROS burst

Seven-day-old seedlings cultivated on half-strength MS agar medium were transferred to gel medium soaked with a solution containing no or 0.75 mM $AlCl_3$ for 12 h. For ROS detection, the roots of the seedlings were stained with 10 μM H_2DCFDA and 50 nM MitoTracker Red for 30 min and were subjected to fluorescence detection after washing twice with 18 MΩ water. For H_2O_2 detection, the roots were incubated in a freshly prepared staining solution composed of 1 mg/mL DAB and 0.1% (v/v) Tween 20 in 10 mM Na_2HPO_4 in the dark for 3 h. For O_2^- detection, 0.5 mg/mL NBT solution was used to stain the roots in the dark for 1 h. The stained roots were observed and photographed using a stereomicroscope (SZX12, Olympus) equipped with a camera (DP20, Olympus).

To determine the rate of mitochondrial H_2O_2 production, a previously described method for isolating root mitochondria was followed (Considine et al. 2003). Briefly, approximately 5 g roots of 10-d-old seedlings treated with no or 0.75 mM $AlCl_3$-soaked gel medium for 12 h were homogenized into 10 mL of extraction medium, consisting of 0.3 M mannitol, 50 mM TES-NaOH (pH 7.5), 0.5% (w/v) BSA, 0.5% (w/v) polyvinylpyrrolidone-40, 2 mM EGTA, and 20 mM cysteine. The resulting homogenate was centrifuged at 1,500 × *g* for 10 min at 4 °C. The supernatant was then subjected to another centrifugation at 18,000 × *g* for 10 min to collect the organelle pellet. This pellet was resuspended in wash buffer composed of 0.3 M mannitol and 20 mM TES-KOH (pH 7.5) and layered onto a stepped Percoll gradient. The Percoll gradient consisted of steps of 50, 28, and 20% (w/v) Percoll with 0.3 M mannitol as an osmoticum. After centrifugation at 43,000 × *g* for 30 min at 4 °C, mitochondria were recovered from the 28% to 50% Percoll interface. Further purification of mitochondria was performed using a second self-forming Percoll gradient consisting of 28% Percoll with 0.3 M sucrose as an osmoticum. Measurement of mitochondrial H_2O_2 was conducted using the peroxidase-dependent conversion of Amplex Red (ST010, Beyotime, China) to resorufin, following the method described by Smith et al. (2004). The assay mixture, with a final volume of 200 μL, contained 50 μM Amplex Red, 10 units superoxide dismutase, 1.2 units of horseradish peroxidase, 0.3 M mannitol, 10 mM TES-KOH (pH 7.5), 3 mM $MgSO_4$, 10 mM NaCl, 5 mM KH_2PO_4, 0.1% (w/v) BSA, 20 mM glucose, 0.3 mM NAD^+, 0.1 mM ADP, 0.1 mM thiamin pyrophosphate, 0.15 units/mL of hexokinase, and purified

mitochondria (100 μg protein equivalent). The background rate of H_2O_2 production was determined by measuring the accumulation rate of resorufin using fluorescence spectrophotometry (excitation at 570 nm, emission at 587 nm). Respiratory substrates including 10 mM pyruvate, 2.1 mM citrate, 1.3 mM succinate, 0.6 mM malate, 0.02 mM fumarate, and 0.02 mM isocitrate were then added, and the rate of H_2O_2 production was measured over a time period of 10 to 15 min after the addition of the substrates.

Determination of protein levels in roots

To assess STOP1 accumulation in different lines, seedlings were grown on gel medium soaked with no $AlCl_3$ or 0.75 mM $AlCl_3$ for 7 d. Subsequently, the roots were excised for protein extraction. To examine the effect of the *rae6* mutation on STOP1 stability, 9-d-old seedlings were pretreated with a 0.5-mM $CaCl_2$ solution at pH 4.8 for 2 h and then exposed to the same $CaCl_2$ solution containing no Al or 30 μM $AlCl_3$ for 4 h. The seedlings subjected to Al treatment were further exposed to the same $CaCl_2$ solution containing 30 μM Al and 100 μM cycloheximide (A8244; ApexBio) for varying time intervals. At each time point, roots were harvested for protein extraction. To investigate the influence of MG132 on STOP1 accumulation, 9-d-old seedlings were exposed to either no Al or 30 μM Al for 3 h and then 50 μM MG132 with no Al or 30 μM Al for 3 h. Subsequently, the roots were collected for protein extraction. To explore the effect of H_2O_2 on STOP1 accumulation, 9-d-old seedlings were exposed to either no or 1 mM H_2O_2 for 3 h, after which the roots were excised for protein extraction. Total proteins were extracted using the protein extraction buffer mentioned above, and were then separated by 8% (w/v) SDS-PAGE. The resolved STOP1-3HA proteins were detected through standard immunoblot assays using HA-HRP antibody. Actin served as a loading control and was detected using an anti-Actin antibody (CW0264M; CoWin Biosciences).

GUS analysis

To determine the STOP1-GUS protein accumulation, 10-d-old seedlings from the wild type and *rae6* carrying the *proSTOP1:STOP1-GUS* transgene were pretreated with a 0.5 mM $CaCl_2$ solution at pH 4.8 for 2 h and then exposed to the same $CaCl_2$ solution containing either no Al or 30 μM Al for 8 h. Subsequently, the roots were collected and ground to a fine powder, which was then mixed with GUS extraction buffer comprising 50 mM sodium phosphate, pH 7.0, 10 mM EDTA, 0.1% (w/v) SDS, 0.1% (v/v) Triton X-100, 10 mM 2-mercaptoethanol, and 25 mg/mL PMSF. The mixed solution was centrifuged at 13,523 × *g* for 10 min at 4 °C, and subsequently a portion of the supernatant was mixed with GUS extraction buffer containing 1 mM 4-methylumbelliferyl β-D-glucuronide (A602251; Sangon Biotech) at 37 °C. After 1 h, a solution of 0.2 M Na_2CO_3 was added to halt the reaction. The fluorescence of the fluorochrome 4-methylumbelliferone in the reaction was measured, with excitation and emission wavelengths of 350 and 455 nm, respectively. GUS activity in each sample was normalized to total protein content.

To generate *proRAE6:GUS* transgenic lines, a 1.5 kb promoter fragment of *RAE6* was amplified and cloned upstream of the *GUS* reporter gene in the pORE-R2 vector. Different tissues from 1 *proRAE6:GUS* transgenic line were stained with a commercialized GUS staining solution (S102; O'Biolab, Beijing, China). Stained tissues were observed and photographed using a stereomicroscope (SZX12, Olympus) equipped with a camera (DP20, Olympus).

Determination of STOP1 oxidation

The oxidation modification assay of Arabidopsis proteins was performed as previously described (Tian et al. 2018). For H_2O_2 treatment, seedlings grown on half-strength MS agar medium for 10 d remained on the same medium or were treated with 1 mM H_2O_2 for 3 h. For Al treatment, the seedlings were grown on gel medium soaked with no $AlCl_3$ or 0.75 mM $AlCl_3$ for 7 d. The roots of the seedlings were harvested and ground to a fine powder in liquid nitrogen. Total proteins were extracted using extraction buffer, consisting of 20 mM HEPES (pH 8.0), 40 mM KCl, 5 mM EDTA, 0.5% (v/v) Triton X-100, 1% (w/v) SDS, 1 mM PMSF, and 1× protease inhibitor cocktail. The protein extracts were incubated with 100 mM NEM in EBR buffer at room temperature for 30 min with frequent vortexing to block free thiols. The samples were then precipitated with 1 volume of acetone and washed 3 times with 50% (v/v) acetone. The pellets were dissolved in 500 μL EBR buffer containing 20 mM DTT and were incubated at 37 °C for 30 min to reduce the oxidized thiols. DTT was removed by protein precipitation with 1 volume of acetone, and the pellets were resuspended in 500 μL EBR buffer. The supernatant was labeled with 100 μM BIAM at room temperature for 1 h in the dark, and proteins were precipitated with 1 volume of acetone to remove free BIAM. The BIAM-treated proteins were then dissolved in 250 μL extraction buffer and diluted with 750 μL incubation buffer, composed of 20 mM HEPES (pH 8.0), 40 mM KCl, 5 mM EDTA, 0.25% (v/v) Triton X-100, 1 mM PMSF, and 1 × protease inhibitor cocktail. After centrifugation at 12,000 × *g* for 5 min at 4 °C, the supernatant was added to 40 μL of streptavidin beads and incubated at 4 °C overnight. The beads were washed 5 times with the incubation buffer, and the proteins were eluted with 40 μL of 2 × SDS sample buffer. The samples were then separated on 8% (w/v) SDS-PAGE gels. An aliquot of proteins before incubation with streptavidin beads was used as total STOP1 protein control. The anti-HA-HRP antibody was used to detect oxidized or total STOP1-HA protein.

For in vitro reduction analysis of STOP1 by TRX1, recombinant STOP1-His and GST-TRX1 were purified from *E. coli*. Subsequently, STOP1-His, pretreated with H_2O_2, was incubated at room temperature for 3 h alone or with a TRX system. The TRX system comprised 0.5 mM NADPH, 1 μM TRX reductase (T7915; Sigma-Aldrich), and 5 μg GST-TRX1. To

precipitate the proteins, 1 volume of acetone was added, and the mixture was kept at −20 °C for 20 min, followed by centrifugation at 5,000 × *g* for 5 min at 4 °C. The resulting pellet was washed 3 times with 50% (v/v) acetone and then dissolved in 500 μL EBR buffer. The in vitro oxidation of STOP1 was detected using the same method as described for the aforementioned in vivo oxidation detection.

LC–MS/MS analysis

Recombinant STOP1 was treated with 1 mM H_2O_2 or DTT for 30 min at room temperature, and was then incubated with 100 mM NEM in EBR buffer at room temperature for 30 min with frequent vortexing to block free thiols. The sample was then precipitated by ice-cold acetone and labeled with 100 μM BIAM at room temperature for 1 h in the dark. The labeled protein was in-gel digested with trypsin, 1:30 (V5280, Promega). The resulting sample was redissolved in a 0.1% (v/v) formic acid solution and adsorbed onto an Easy column with an injection needle (SenSil C18-AQ, 75 μm × 25 cm, 1.6 μm) from Fresh Bioscience. Separation was carried out using an EASY-nLC 1200 liquid phase system (Thermo Scientific). Mobile phase A consisted of a 0.1% (v/v) formic acid aqueous solution, while mobile phase B consisted of an 80% (v/v) acetonitrile with 0.1% (v/v) formic acid. Gradient elution was performed at a flow rate of 250 nL/min for 75 min. The samples were separated by chromatography and then analyzed by mass spectrometry using a Q EXACTIVE HF instrument (Thermo Scientific). The source voltage was set to 2.4 kV, and the parent ions and secondary fragments of the peptides were detected and analyzed using a high-resolution Orbitrap. For primary mass spectrometry, the scanning range was set from 300 to 1,650 *m/z* with a scanning resolution of 45,000. For secondary mass spectrometry, the scanning range was fixed to 100 *m/z*, and the scanning resolution of the Orbitrap was set to 30,000. The data acquisition mode employed a data-dependent acquisition program, which selected the 20 parent ions with the highest signal intensity for higher-energy collisional dissociation. A fragmentation energy of 32% was used for fragmentation. Likewise, secondary mass spectrometry was performed successively. To enhance mass spectrum utilization efficiency, the automatic gain control was set to 200,000 the maximum injection time was set to 100 ms, and a dynamic exclusion time of 30 s was implemented during series mass spectrum scanning to prevent repeated scanning of parent ions.

In vitro BIAM-labeling and STOP1 oxidation assays

For the BIAM-labeling assay, recombinant STOP1-His and $STOP1^{3CS}$-His proteins were treated with different concentrations of H_2O_2 at room temperature for 15 min. The proteins were precipitated by adding 1 volume of acetone at −20 °C for 20 min and then centrifuged at 5,000 × *g* for 5 min at 4 °C. The pellets were washed 3 times with 50% (v/v) acetone and dissolved in 500 μL of labeling buffer containing 50 mM MES-NaOH (pH6.5), 100 mM NaCl, 1% (v/v) Triton X-100, and 100 μM BIAM. They were then incubated at room temperature in the dark for 1 h. The labeling reactions were terminated by adding β-mercaptoethanol to a final concentration of 20 mM. The reaction mixtures were precipitated by adding 1 volume of acetone at −20 °C for 20 min and then centrifuged at 5,000 × *g* for 5 min at 4 °C. The pellets were dissolved in 40 μL of SDS sample buffer, and subjected to separate on SDS-PAGE. Proteins labeled with BIAM were detected using HRP-conjugated streptavidin (SLP001H, Smart-Lifesciences).

For in vitro oxidation analysis, recombinant STOP1-His, $STOP1^{C8S}$-His, $STOP1^{C27S}$-His, $STOP1^{C185S}$-His, and $STOP1^{3CS}$-His proteins were purified from *E. coli* and then treated with 1 mM H_2O_2 or 1 mM DTT at room temperature for 15 min. The proteins were precipitated by adding 1 volume of acetone at −20 °C for 20 min and then centrifuged at 5,000 × *g* for 5 min at 4 °C. The pellet was washed 3 times with 50% (v/v) acetone and dissolved in 500 μL EBR buffer. The in vitro oxidation state of STOP1 was then detected using the same method as the aforementioned in vivo oxidation detection.

Quantification and statistical analysis

ImageJ software was used to quantify the band intensities from immunoblots or the intensity of fluorescence and chemical staining. Statistical analysis between 2 groups was conducted using a 2-tailed Student's *t* test; when more than 2 groups were involved, a 1-way analysis of variance (ANOVA) followed by Tukey test was performed using GraphPad Prism 9.00 software. Statistical data are provided in Supplemental Data Set 2.

Accession numbers

Gene sequence data in this article can be found in the Arabidopsis Information Resource (TAIR) database under the following accession numbers: At1g34370 (*STOP1*), At1g08430 (*ALMT1*), At1g51340 (*MATE*), At2g37330 (*ALS3*), At1g67940 (*STAR1*), At5g39040 (*ALS1*), At1g73710 (*RAE6*), At2g37330 (*ALS3*), At4g35090 (*CAT2*), At5g47910 (*RBOHD*), At5g01720 (*RAE1*), and At3g51030 (*TRX1*). Whole-genome sequence data of pooled F_2 *rae6* mutant plants produced in this study were deposited at the National Center for Biotechnology Information (accession number: SRR17165106).

Acknowledgments

We thank Prof. Ian Small from The University of Western Australia for commenting on RAE6 function.

Author contributions

X.W., Y.Z., and C.-F.H. designed the experiments. X.W., Y.Z., W.X., W.R., Y.Z., and H.Z. performed the experiments. S.D. commented on the research. X.W. and C.-F.H. wrote the manuscript.

Supplemental data

The following materials are available in the online version of this article.

Supplemental Figure S1. Effect of the *rae6* mutation on the expression of Al resistance genes and plant development.

Supplemental Figure S2. MutMap analysis of the *rae6* mutant.

Supplemental Figure S3. Genetic rescue of the *rae6* mutant.

Supplemental Figure S4. Effect of *RAE6* knockout or knockdown on plant development, the expression of STOP1-regulated genes, and Al resistance.

Supplemental Figure S5. Expression pattern of *RAE6*.

Supplemental Figure S6. Effect of the *rae6* mutation on the expression of mitochondrial genes.

Supplemental Figure S7. Exogenous supply of GSH partially rescues the Al-sensitive phenotype and expression of STOP1-regulated genes of *rae6*.

Supplemental Figure S8. Mutation of *RBOHD* rescues the Al-sensitive phenotype, and decreased STOP1 accumulation and expression of STOP1-regulated genes in *rae6*.

Supplemental Figure S9. Mass spectrometry analysis of the tryptic fragments of STOP1-His.

Supplemental Figure S10. Triple C-to-S mutations (3CS) of C8, C27, and C185 of STOP1 increase the expression of STOP1-regulated genes and rescue the Al-sensitive phenotype of *rae6*.

Supplemental Figure S11. Mutation of *RAE1* rescues the *rae6*-induced decreased expression of STOP1-regulated genes.

Supplemental Figure S12. Rescue of *trx1* deficiency by wild-type *TRX1* and triple C-to-S mutations (3CS) of C8, C27, and C185 in STOP1.

Supplemental Table S1. List of mutations in the *rae6* mutant and linkage analysis.

Supplemental Data Set 1. Primers used in this study.

Supplemental Data Set 2. Summary of statistical analyses in all figures.

Funding

This work was supported by the National Natural Science Foundation of China (Grant No. 32170261 to C.-F.H.) and by National Key Laboratory of Plant Molecular Genetics.

Conflict of interest statement. None declared.

References

Abe A, Kosugi S, Yoshida K, Natsume S, Takagi H, Kanzaki H, Matsumura H, Mitsuoka C, Tamiru M, Innan H, et al. Genome sequencing reveals agronomically important loci in rice using MutMap. Nat Biotechnol. 2012:**30**(2):174–178. https://doi.org/10.1038/nbt.2095

Balzergue C, Dartevelle T, Godon C, Laugier E, Meisrimler C, Teulon JM, Creff A, Bissler M, Brouchoud C, Hagege A, et al. Low phosphate activates STOP1-ALMT1 to rapidly inhibit root cell elongation. Nat Commun. 2017:**8**(1):15300. https://doi.org/10.1038/ncomms15300

Barkan A, Small I. Pentatricopeptide repeat proteins in plants. Annu. Rev. Plant Biol. 2014:**65**(1):415–442. https://doi.org/10.1146/annurev-arplant-050213-040159

Bienert GP, Schjoerring JK, Jahn TP. Membrane transport of hydrogen peroxide. Bba-Biomembranes. 2006:**1758**(8):994–1003. https://doi.org/10.1016/j.bbamem.2006.02.015

Bonen L. Cis- and trans-splicing of group II introns in plant mitochondria. Mitochondrion. 2008:**8**(1):26–34. https://doi.org/10.1016/j.mito.2007.09.005

Castro B, Citterico M, Kimura S, Stevens DM, Wrzaczek M, Coaker G. Stress-induced reactive oxygen species compartmentalization, perception and signalling. Nat Plants. 2021:**7**(4):403–412. https://doi.org/10.1038/s41477-021-00887-0

Colas des Francs-Small C, Falcon de Longevialle A, Li Y, Lowe E, Tanz SK, Smith C, Bevan MW, Small I. The pentatricopeptide repeat proteins TANG2 and ORGANELLE TRANSCRIPT PROCESSING439 are involved in the splicing of the multipartite *nad5* transcript encoding a subunit of mitochondrial complex I. Plant Physiol. 2014:**165**(4):1409–1416. https://doi.org/10.1104/pp.114.244616

Considine MJ, Goodman M, Echtay KS, Laloi M, Whelan J, Brand MD, Sweetlove LJ. Superoxide stimulates a proton leak in potato mitochondria that is related to the activity of uncoupling protein. J Biol Chem. 2003:**278**(25):22298–22302. https://doi.org/10.1074/jbc.M301075200

Enomoto T, Tokizawa M, Ito H, Iuchi S, Kobayashi M, Yamamoto YY, Kobayashi Y, Koyama H. STOP1 regulates the expression of *HsfA2* and *GDHs* that are critical for low-oxygen tolerance in Arabidopsis. J Exp Bot. 2019:**70**(12):3297–3311. https://doi.org/10.1093/jxb/erz124

Fang Q, Zhang J, Yang DL, Huang CF. The SUMO E3 ligase SIZ1 partially regulates STOP1 SUMOylation and stability in *Arabidopsis thaliana*. Plant Signal. Behav. 2021a:**16**(5):1899487. https://doi.org/10.1080/15592324.2021.1899487

Fang Q, Zhang J, Zhang Y, Fan N, van den Burg HA, Huang CF. Regulation of aluminum resistance in *Arabidopsis* involves the SUMOylation of the zinc finger transcription factor STOP1. Plant Cell. 2020:**32**(12):3921–3938. https://doi.org/10.1105/tpc.20.00687

Fang Q, Zhou F, Zhang Y, Singh S, Huang CF. Degradation of STOP1 mediated by the F-box proteins RAH1 and RAE1 balances aluminum resistance and plant growth in *Arabidopsis thaliana*. Plant J. 2021b:**106**(2):493–506. https://doi.org/10.1111/tpj.15181

Fujii S, Small I. The evolution of RNA editing and pentatricopeptide repeat genes. New Phytol. 2011:**191**(1):37–47. https://doi.org/10.1111/j.1469-8137.2011.03746.x

Fujiwara T, Hirai MY, Chino M, Komeda Y, Naito S. Effects of sulfur nutrition on expression of the soybean seed storage protein genes in transgenic petunia. Plant Physiol. 1992:**99**(1):263–268. https://doi.org/10.1104/pp.99.1.263

Garcia-Santamarina S, Boronat S, Hidalgo E. Reversible cysteine oxidation in hydrogen peroxide sensing and signal transduction. Biochemistry-Us. 2014:**53**(16):2560–2580. https://doi.org/10.1021/bi401700f

Guo J, Zhang Y, Gao H, Li S, Wang ZY, Huang CF. Mutation of *HPR1* encoding a component of the THO/TREX complex reduces STOP1 accumulation and aluminium resistance in *Arabidopsis thaliana*. New Phytol. 2020:**228**(1):179–193. https://doi.org/10.1111/nph.16658

Hampp R, Goller M, Fullgraf H. Determination of compartmented metabolite pools by a combination of rapid fractionation of oat mesophyll protoplasts and enzymic cycling. Plant Physiol. 1984:**75**(4):1017–1021. https://doi.org/10.1104/pp.75.4.1017

Heazlewood JL, Howell KA, Millar AH. Mitochondrial complex I from Arabidopsis and rice: orthologs of mammalian and fungal components coupled with plant-specific subunits. Biochim. Biophys. Acta. 2003:**1604**(3):159–169. https://doi.org/10.1016/S0005-2728(03)00045-8

Huang WJ, Yang XD, Yao SC, LwinOo T, He HY, Wang AQ, Li CZ, He LF. Reactive oxygen species burst induced by aluminum stress triggers mitochondria-dependent programmed cell death in peanut root tip cells. Plant Physiol. Bioch. 2014:**82**:76–84. https://doi.org/10.1016/j.plaphy.2014.03.037

Iuchi S, Koyama H, Iuchi A, Kobayashi Y, Kitabayashi S, Ikka T, Hirayama T, Shinozaki K, Kobayashi M. Zinc finger protein STOP1 is critical for proton tolerance in *Arabidopsis* and coregulates a key gene in aluminum tolerance. Proc Natl Acad Sci USA. 2007:**104**(23):9900–9905. https://doi.org/10.1073/pnas.0700117104

Kelly BM, Wiskich JT. Respiration of mitochondria isolated from leaves and protoplasts of *Avena sativa*. Plant Physiol. 1988:**87**(3):705–710. https://doi.org/10.1104/pp.87.3.705

Kim JR, Yoon HW, Kwon KS, Lee SR, Rhee SG. Identification of proteins containing cysteine residues that are sensitive to oxidation by hydrogen peroxide at neutral pH. Anal Biochem. 2000:**283**(2):214–221. https://doi.org/10.1006/abio.2000.4623

Kochian LV. Cellular mechanisms of aluminum toxicity and resistance in plants. Annu Rev Plant Physiol Plant Mol Biol. 1995:**46**(1):237–260. https://doi.org/10.1146/annurev.pp.46.060195.001321

Kochian LV, Pineros MA, Liu JP, Magalhaes JV. Plant adaptation to acid soils: the molecular basis for crop aluminum resistance. Annu. Rev. Plant Biol. 2015:**66**(1):571–598. https://doi.org/10.1146/annurev-arplant-043014-114822

Larsen PB, Geisler MJB, Jones CA, Williams KM, Cancel JD. ALS3 encodes a phloem-localized ABC transporter-like protein that is required for aluminum tolerance in Arabidopsis. Plant J. 2005:**41**(3):353–363. https://doi.org/10.1111/j.1365-313X.2004.02306.x

Lee ES, Park JH, Wi SD, Kang CH, Chi YH, Chae HB, Paeng SK, Ji MG, Kim WY, Kim MG, et al. Redox-dependent structural switch and CBF activation confer freezing tolerance in plants. Nat Plants. 2021:**7**(7):914. https://doi.org/10.1038/s41477-021-00944-8

Leu KC, Hsieh MH, Wang HJ, Hsieh HL, Jauh GY. Distinct role of *Arabidopsis* mitochondrial P-type pentatricopeptide repeat protein-modulating editing protein, PPME, in *nad1* RNA editing. RNA Biol. 2016:**13**(6):593–604. https://doi.org/10.1080/15476286.2016.1184384

Li R, Kast J. Biotin switch assays for quantitation of reversible cysteine oxidation. Methods Enzymol. 2017:**585**:269–284. https://doi.org/10.1016/bs.mie.2016.10.006

Ligaba-Osena A, Fei ZJ, Liu JP, Xu YM, Shaff J, Lee SC, Luan S, Kudla J, Kochian L, Pineros M. Loss-of-function mutation of the calcium sensor CBL1 increases aluminum sensitivity in *Arabidopsis*. New Phytol. 2017:**214**(2):830–841. https://doi.org/10.1111/nph.14420

Liu JP, Magalhaes JV, Shaff J, Kochian LV. Aluminum-activated citrate and malate transporters from the MATE and ALMT families function independently to confer *Arabidopsis* aluminum tolerance. Plant J. 2009:**57**(3):389–399. https://doi.org/10.1111/j.1365-313X.2008.03696.x

Liu Y, He JN, Chen ZZ, Ren XZ, Hong XH, Gong ZZ. *ABA overly-sensitive 5* (*ABO5*), encoding a pentatricopeptide repeat protein required for cis-splicing of mitochondrial *nad2* intron 3, is involved in the abscisic acid response in Arabidopsis. Plant J. 2010:**63**(5):749–765. https://doi.org/10.1111/j.1365-313X.2010.04280.x

Lu Q, Houbaert A, Ma Q, Huang JJ, Sterck L, Zhang C, Benjamins R, Coppens F, Van Breusegem F, Russinova E. Adenosine monophosphate deaminase modulates BIN2 activity through hydrogen peroxide-induced oligomerization. Plant Cell. 2022:**34**(10):3844–3859. https://doi.org/10.1093/plcell/koac203

Ma BH, Wan JM, Shen ZG. H_2o_2 production and antioxidant responses in seeds and early seedlings of two different rice varieties exposed to aluminum. Plant Growth Regul. 2007:**52**(1):91–100. https://doi.org/10.1007/s10725-007-9183-1

Ma JF. Syndrome of aluminum toxicity and diversity of aluminum resistance in higher plants. Int Rev Cytol. 2007:**264**:225–252. https://doi.org/10.1016/S0074-7696(07)64005-4

Marinho HS, Real C, Cyrne L, Soares H, Antunes F. Hydrogen peroxide sensing, signaling and regulation of transcription factors. Redox Biol. 2014:**2**:535–562. https://doi.org/10.1016/j.redox.2014.02.006

Matsumoto H, Motoda H. Oxidative stress is associated with aluminum toxicity recovery in apex of pea root. Plant Soil. 2013:**363**(1–2):399–410. https://doi.org/10.1007/s11104-012-1396-z

Maxwell DP, Wang Y, McIntosh L. The alternative oxidase lowers mitochondrial reactive oxygen production in plant cells. Proc Natl Acad Sci USA. 1999:**96**(14):8271–8276. https://doi.org/10.1073/pnas.96.14.8271

Meyer Y, Belin C, Delorme-Hinoux V, Reichheld JP, Riondet C. Thioredoxin and glutaredoxin systems in plants: molecular mechanisms, crosstalks, and functional significance. Antioxid. Redox Sign. 2012:**17**(8):1124–1160. https://doi.org/10.1089/ars.2011.4327

Mittler R, Zandalinas SI, Fichman Y, Van Breusegem F. Reactive oxygen species signalling in plant stress responses. Nat Rev Mol Cell Biol. 2022:**23**(10):663–679. https://doi.org/10.1038/s41580-022-00499-2

Moller IM. Plant mitochondria and oxidative stress: electron transport, NADPH turnover, and metabolism of reactive oxygen species. Annu Rev Plant Physiol Plant Mol Biol. 2001:**52**(1):561–591. https://doi.org/10.1146/annurev.arplant.52.1.561

Moller IM, Jensen PE, Hansson A. Oxidative modifications to cellular components in plants. Annu. Rev. Plant Biol. 2007:**58**(1):459–481. https://doi.org/10.1146/annurev.arplant.58.032806.103946

Mora-Macias J, Ojeda-Rivera JO, Gutierrez-Alanis D, Yong-Villalobos L, Oropeza-Aburto A, Raya-Gonzalez J, Jimenez-Dominguez G, Chavez-Calvillo G, Rellan-Alvarez R, Herrera-Estrella L. Malate-dependent Fe accumulation is a critical checkpoint in the root developmental response to low phosphate. Proc Natl Acad Sci USA. 2017:**114**(17):E3563–E3572. https://doi.org/10.1073/pnas.1701952114

Mou Z, Fan WH, Dong XN. Inducers of plant systemic acquired resistance regulate NPR1 function through redox changes. Cell. 2003:**113**(7):935–944. https://doi.org/10.1016/S0092-8674(03)00429-X

Nakano Y, Kusunoki K, Hoekenga OA, Tanaka K, Iuchi S, Sakata Y, Kobayashi M, Yamamoto YY, Koyama H, Kobayashi Y. Genome-wide association study and genomic prediction elucidate the distinct genetic architecture of aluminum and proton tolerance in *Arabidopsis thaliana*. Front. Plant Sci. 2020:**11**:405. https://doi.org/10.3389/fpls.2020.00405

Peleg-Grossman S, Melamed-Book N, Cohen G, Levine A. Cytoplasmic H_2O_2 prevents translocation of NPR1 to the nucleus and inhibits the induction of PR genes in Arabidopsis. Plant Signal. Behav. 2010:**5**(11):1401–1406. https://doi.org/10.4161/psb.5.11.13209

Poschenrieder C, Gunse B, Corrales I, Barcelo J. A glance into aluminum toxicity and resistance in plants. Sci. Total Environ. 2008:**400**(1–3):356–368. https://doi.org/10.1016/j.scitotenv.2008.06.003

Sadhukhan A, Enomoto T, Kobayashi Y, Watanabe T, Iuchi S, Kobayashi M, Sahoo L, Yamamoto YY, Koyama H. Sensitive to Proton Rhizotoxicity1 regulates salt and drought tolerance of *Arabidopsis thaliana* through transcriptional regulation of *CIPK23*. Plant Cell Physiol. 2019:**60**(9):2113–2126. https://doi.org/10.1093/pcp/pcz120

Sadhukhan A, Kobayashi Y, Iuchi S, Koyama H. Synergistic and antagonistic pleiotropy of STOP1 in stress tolerance. Trends Plant Sci. 2021:**26**(10):1014–1022. https://doi.org/10.1016/j.tplants.2021.06.011

Sawaki Y, Iuchi S, Kobayashi Y, Kobayashi Y, Ikka T, Sakurai N, Fujita M, Shinozaki K, Shibata D, Kobayashi M, et al. STOP1 regulates multiple genes that protect Arabidopsis from proton and aluminum toxicities. Plant Physiol. 2009:**150**(1):281–294. https://doi.org/10.1104/pp.108.134700

Schmidt R, Schippers JHM. ROS-mediated redox signaling during cell differentiation in plants. Bba-Gen Subjects. 2015:**1850**(8):1497–1508. https://doi.org/10.1016/j.bbagen.2014.12.020

Schmitz-Linneweber C, Small I. Pentatricopeptide repeat proteins: a socket set for organelle gene expression. Trends Plant Sci. 2008:**13**(12):663–670. https://doi.org/10.1016/j.tplants.2008.10.001

Shaikhali J, Noren L, de Dios Barajas-Lopez J, Srivastava V, Konig J, Sauer UH, Wingsle G, Dietz KJ, Strand A. Redox-mediated mechanisms regulate DNA binding activity of the G-group of basic region

leucine zipper (bZIP) transcription factors in *Arabidopsis*. J Biol Chem. 2012:**287**(33):27510–27525. https://doi.org/10.1074/jbc.M112.361394

Smith AM, Ratcliffe RG, Sweetlove LJ. Activation and function of mitochondrial uncoupling protein in plants. J Biol Chem. 2004:**279**(50):51944–51952. https://doi.org/10.1074/jbc.M408920200

Sugiyama Y, Watase Y, Nagase M, Makita N, Yagura S, Hirai A, Sugiura M. The complete nucleotide sequence and multipartite organization of the tobacco mitochondrial genome: comparative analysis of mitochondrial genomes in higher plants. Mol Genet Genomics. 2005:**272**(6):603–615. https://doi.org/10.1007/s00438-004-1075-8

Tahara K, Yamanoshita T, Norisada M, Hasegawa I, Kashima H, Sasaki S, Kojima K. Aluminum distribution and reactive oxygen species accumulation in root tips of two *Melaleuca* trees differing in aluminum resistance. Plant Soil. 2008:**307**(1–2):167–178. https://doi.org/10.1007/s11104-008-9593-5

Tamas L, Simonovicova M, Huttova J, Mistrik I. Aluminium stimulated hydrogen peroxide production of germinating barley seeds. Environ Exp Bot. 2004:**51**(3):281–288. https://doi.org/10.1016/j.envexpbot.2003.11.007

Tian WH, Ye JY, Cui MQ, Chang JB, Liu Y, Li GX, Wu YR, Xu JM, Harberd NP, Mao CZ, et al. A transcription factor STOP1-centered pathway coordinates ammonium and phosphate acquisition in *Arabidopsis*. Mol Plant. 2021:**14**(9):1554–1568. https://doi.org/10.1016/j.molp.2021.06.024

Tian YC, Fan M, Qin ZX, Lv HJ, Wang MM, Zhang Z, Zhou WY, Zhao N, Li XH, Han C, et al. Hydrogen peroxide positively regulates brassinosteroid signaling through oxidation of the BRASSINAZOLE-RESISTANT1 transcription factor. Nat Commun. 2018:**9**(1):1063. https://doi.org/10.1038/s41467-018-03463-x

Tokizawa M, Enomoto T, Ito H, Wu L, Kobayashi Y, Mora-Macias J, Armenta-Medina D, Iuchi S, Kobayashi M, Nomoto M, et al. High affinity promoter binding of STOP1 is essential for early expression of novel aluminum-induced resistance genes *GDH1* and *GDH2* in Arabidopsis. J Exp Bot. 2021:**72**(7):2769–2789. https://doi.org/10.1093/jxb/erab031

Vanlerberghe GC. Alternative oxidase: a mitochondrial respiratory pathway to maintain metabolic and signaling homeostasis during abiotic and biotic stress in plants. Int J Mol Sci. 2013:**14**(4):6805–6847. https://doi.org/10.3390/ijms14046805

von Uexkull HR, Mutert E. Global extent, development and economic-impact of acid soils. Plant Soil. 1995:**171**(1):1–15. https://doi.org/10.1007/BF00009558

Wang C, Aube F, Quadrado M, Dargel-Graffin C, Mireau H. Three new pentatricopeptide repeat proteins facilitate the splicing of mitochondrial transcripts and complex I biogenesis in Arabidopsis. J Exp Bot. 2018:**69**(21):5131–5140. https://doi.org/10.1093/jxb/ery275

Wang ZF, Mi TW, Gao YQ, Feng HQ, Wu WH, Wang Y. STOP1 regulates *LKS1* transcription and coordinates K^+/NH_4^+ balance in *Arabidopsis* response to Low-K^+ stress. Int J Mol Sci. 2022:**23**(1):383. https://doi.org/10.3390/ijms23010383

Wei C, Wang C, Jia M, Guo HX, Luo PY, Wang MG, Zhu JK, Zhang H. Efficient generation of homozygous substitutions in rice in one generation utilizing an rABE8e base editor. J. Integr. Plant Biol. 2021:**63**(9):1595–1599. https://doi.org/10.1111/jipb.13089

Xu J, Zhu J, Liu J, Wang J, Ding Z, Tian H. SIZ1 negatively regulates aluminum resistance by mediating the STOP1-ALMT1 pathway in *Arabidopsis*. J. Integr. Plant Biol. 2021:**63**(6):1147–1160. https://doi.org/10.1111/jipb.13091

Yamamoto Y, Kobayashi Y, Devi SR, Rikiishi S, Matsumoto H. Aluminum toxicity is associated with mitochondrial dysfunction and the production of reactive oxygen species in plant cells. Plant Physiol. 2002:**128**(1):63–72. https://doi.org/10.1104/pp.010417

Yang Y, Zhao Y, Zhang YQ, Niu LH, Li WY, Lu WQ, Li JF, Schafer P, Meng YL, Shan WX. A mitochondrial RNA processing protein mediates plant immunity to a broad spectrum of pathogens by modulating the mitochondrial oxidative burst. Plant Cell. 2022:**34**(6):2343–2363. https://doi.org/10.1093/plcell/koac082

Yuan H, Liu D. Functional disruption of the pentatricopeptide protein SLG1 affects mitochondrial RNA editing, plant development, and responses to abiotic stresses in Arabidopsis. Plant J. 2012:**70**(3):432–444. https://doi.org/10.1111/j.1365-313X.2011.04883.x

Zhai Z, Jung HI, Vatamaniuk OK. Isolation of protoplasts from tissues of 14-day-old seedlings of *Arabidopsis thaliana*. J Vis Exp. 2009:**30**:1149. https://doi.org/10.3791/1149

Zhan J, Li W, He HY, Li CZ, He LF. Mitochondrial alterations during Al-induced PCD in peanut root tips. Plant Physiol. Bioch. 2014:**75**:105–113. https://doi.org/10.1016/j.plaphy.2013.12.010

Zhang Y, Zhang J, Guo JL, Zhou FL, Singh S, Xu X, Xie Q, Yang ZB, Huang CF. F-box protein RAE1 regulates the stability of the aluminum-resistance transcription factor STOP1 in *Arabidopsis*. Proc Natl Acad Sci USA. 2019:**116**(1):319–327. https://doi.org/10.1073/pnas.1814426116

Zhou F, Singh S, Zhang J, Fang Q, Li C, Wang J, Zhao C, Wang P, Huang CF. The MEKK1–MKK1/2–MPK4 cascade phosphorylates and stabilizes STOP1 to confer aluminum resistance in *Arabidopsis*. Mol Plant. 2023:**16**(2):337–353. https://doi.org/10.1016/j.molp.2022.11.010

Zhu Q, Dugardeyn J, Zhang C, Muhlenbock P, Eastmond PJ, Valcke R, De Coninck B, Oden S, Karampelias M, Cammue BP, et al. The *Arabidopsis thaliana* RNA editing factor SLO2, which affects the mitochondrial electron transport chain, participates in multiple stress and hormone responses. Mol Plant. 2014:**7**(2):290–310. https://doi.org/10.1093/mp/sst102

Zhu Q, Dugardeyn J, Zhang C, Takenaka M, Kuhn K, Craddock C, Smalle J, Karampelias M, Denecke J, Peters J, et al. SLO2, a mitochondrial pentatricopeptide repeat protein affecting several RNA editing sites, is required for energy metabolism. Plant J. 2012:**71**(5):836–849. https://doi.org/10.1111/j.1365-313X.2012.05036.x

Zsigmond L, Szepesi A, Tari I, Rigo G, Kiraly A, Szabados L. Overexpression of the mitochondrial *PPR40* gene improves salt tolerance in Arabidopsis. Plant Sci. 2012:**182**:87–93. https://doi.org/10.1016/j.plantsci.2011.07.008